AD-A065 590 OHIO STATE UNIV COLUMBUS ELECTROSCIENCE LAB F/G 9/5
AN ITERATIVE APPROACH FOR COMPUTING AN ANTENNA APERTURE DISTRIB--ETC(U)
JUN 78 E L PELTON, R J MARHEFKA, W D BURNSIDE N62269-76-C-0554
UNCLASSIFIED ESL-(78)4583-6 NADC-79045-30 NL

| OF |
AD
A0 65590

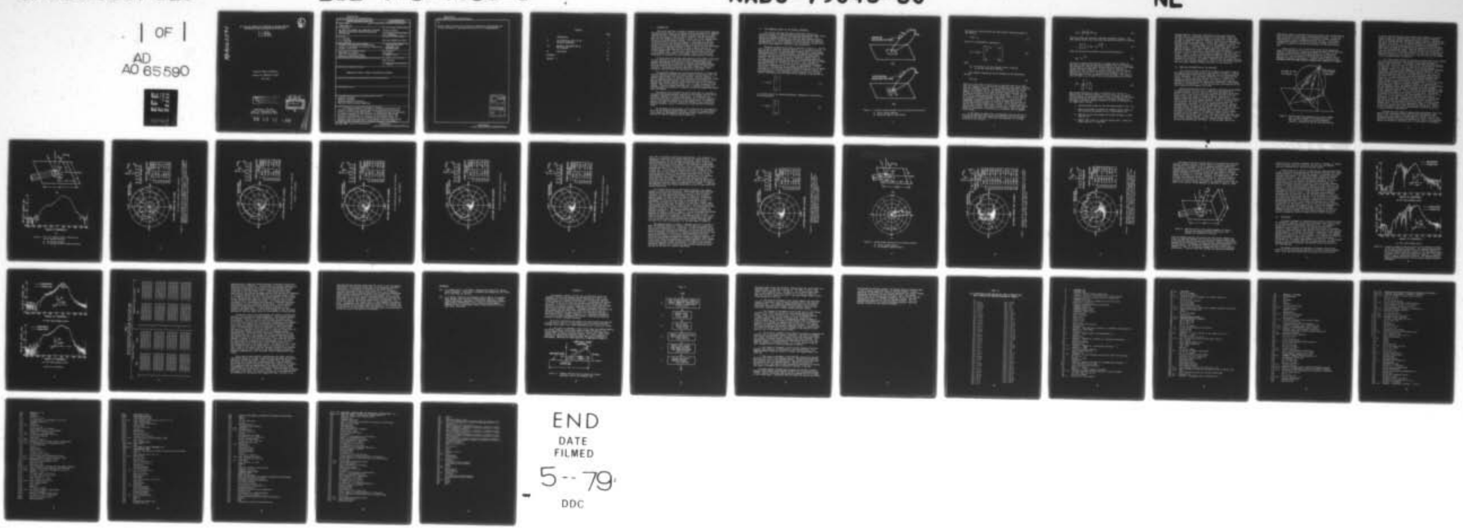

END
DATE
FILMED
5--79
DDC

AD-A065590

AN ITERATIVE APPROACH FOR COMPUTING AN ANTENNA APERTURE DISTRIBUTION FROM GIVEN RADIATION PATTERN DATA

E. L. Pelton
R. J. Marhefka
W. D. Burnside

Technical Report (78)4583-6

Contract No. N62269-76-C-0554

June 1978

Department of the Navy
Naval Air Development Center
Warminster, Pennsylvania 18974

UNCLASSIFIED

SECURITY CLASSIFICATION OF THIS PAGE (When Data Entered)

REPORT DOCUMENTATION PAGE		READ INSTRUCTIONS BEFORE COMPLETING FORM
1. REPORT NUMBER NADC-79045-30	2. GOVT ACCESSION NO.	3. RECIPIENT'S CATALOG NUMBER
4. TITLE (and Subtitle) AN ITERATIVE APPROACH FOR COMPUTING AN ANTENNA APERTURE DISTRIBUTION FROM GIVEN RADIATION PATTERN DATA		5. TYPE OF REPORT & PERIOD COVERED Technical Report 6. PERFORMING ORG. REPORT NUMBER ESL (78)4583-6
7. AUTHOR(s) E. L. Pelton R. J. Marhefka W. D. Burnside		8. CONTRACT OR GRANT NUMBER(s) Contract N62269-76-C-0554
9. PERFORMING ORGANIZATION NAME AND ADDRESS The Ohio State University ElectroScience Laboratory, Department of Electrical Engineering Columbus, Ohio 43212		10. PROGRAM ELEMENT, PROJECT, TASK AREA & WORK UNIT NUMBERS 63206N,WR6-1154 WTW180000,RA702
11. CONTROLLING OFFICE NAME AND ADDRESS Department of the Navy Naval Air Development Center Warminster, Pennsylvania 18974		12. REPORT DATE June 1978 13. NUMBER OF PAGES 41
14. MONITORING AGENCY NAME & ADDRESS(if different from Controlling Office)		15. SECURITY CLASS. (of this report) Unclassified 15a. DECLASSIFICATION/DOWNGRADING SCHEDULE

16. DISTRIBUTION STATEMENT (of this Report)

Approved for public release; distribution unlimited

17. DISTRIBUTION STATEMENT (of the abstract entered in Block 20, if different from Report)

18. SUPPLEMENTARY NOTES

19. KEY WORDS (Continue on reverse side if necessary and identify by block number)

Synthesis procedure
Numerical iteration
Computed aperture distribution
Measured radiation pattern magnitude

20. ABSTRACT (Continue on reverse side if necessary and identify by block number)

An iterative synthesis procedure is presented and applied to the problem of computing the complex aperture distribution of an antenna, given its far field magnitude pattern. The methods employed are applicable to antennas composed of either discrete or continuously distributed apertures, flush-mounted in a finite or infinite ground plane. The solutions obtainable with the procedure are particularly useful for subsequent numerical computation of an antenna's radiation pattern performance, when introduced into a different structural environment.

DD FORM 1 JAN 73 1473 EDITION OF 1 NOV 65 IS OBSOLETE

UNCLASSIFIED

SECURITY CLASSIFICATION OF THIS PAGE (When Data Entered)

20.

Several example solutions are presented to demonstrate the procedure and to point out specific techniques found useful in its implementation.

CONTENTS

I. INTRODUCTION

This report describes a synthesis procedure for efficiently computing the aperture distribution of an antenna based on knowledge of its measured radiation pattern. Although the methods considered are generally applicable to the problem of antenna pattern synthesis, they are considered here from the standpoint of providing a useful tool in the computer-aided design of on-aircraft antenna systems. As a first step in a typical on-aircraft antenna problem, the designer is confronted with the task of selecting one or more candidate antenna configurations which show promise of providing the desired performance in the on-aircraft environment. The selection of candidate antennas is usually made by analysis of measured pattern data taken with the antenna in isolation or mounted in a finite ground plane. Traditionally, the antenna designer tests each of the antennas on an actual or scale-model aircraft, and after many measurements a suitable on-aircraft antenna system eventually evolves.

In recent years it has often been possible to use computer simulation to carry out much of the detailed on-aircraft antenna design. Such computer aided designs have typically relied on assumed approximate aperture distributions to analytically represent the candidate antenna, since the detailed distribution for the actual antenna is usually not available. The synthesis procedure described in the present report provides an efficient means for overcoming this difficulty.

The approaches employed are, with some modifications, an adaptation of basic synthesis techniques presented by Mautz and Harrington [1]. The viewpoint here differs from the usual synthesis situation, however, in that the desired pattern is assumed to be actual and available data, rather than an idealized specification. More specifically the procedure as employed here requires detailed pattern magnitude data for the candidate antenna, taken in the principal planes (i.e., E- and/or H-planes) of the antenna. Since only pattern magnitude data is assumed to be given, an iterative numerical procedure is required to evolve the unspecified pattern phase information.

The methods to be discussed are equally applicable to continuous or discretely distributed aperture antennas, and the antenna aperture may be isolated or mounted in a finite ground plane. For simplicity, the discussion specifically considers the antennas to be linearly polarized, with a planar aperture mounted in a planar ground plane. The methods, however, are general and could readily be extended to treat arbitrarily polarized antennas, as well as arbitrarily curved apertures and ground planes.

The following section presents a brief discussion of the theoretical basis for the synthesis methods employed. Section III discusses details of its numerical implementation and presents several example solutions obtained for specific measured antenna geometries.

II. THE THEORETICAL BASIS OF THE SYNTHESIS PROCEDURE

This section discusses the general theoretical aspects of a synthesis procedure for computing the aperture amplitude and phase distribution of an antenna, given its far-field magnitude pattern. The theoretical approaches employed are similar to those reported by Mautz and Harrington [1]. The subsequently discussed (Section III) numerical implementation of the basic procedure is more specifically geared to our application requirements as outlined in the Introduction.

The general problem to be solved is depicted in Figure 1a. Starting with a given or specified radiation pattern, it is desired to find an aperture distribution (in both amplitude and phase) whose field suitably approximates the given radiation pattern. The aperture distribution may be either discrete or continuously distributed and the ground plane containing the aperture may be finite (including no ground plane) or infinite. For the purposes of analysis, both the computed source (i.e., the computed aperture distribution) and its resulting field are considered to be representable by discrete sets of values. This situation is depicted in Figure 1b. If the true source is continuously distributed the discrete representation is, of course, an approximation. If the true source is discrete the discrete representation may be exact in theory (although any of a multitude of factors would, in practice, prevent an exact realization). The N elemental sources (actually their relative weights) representing the true source can be expressed in matrix form as

$$f = [f_n] = \begin{bmatrix} f_1 \\ f_2 \\ \cdot \\ \cdot \\ \cdot \\ f_N \end{bmatrix} \tag{1}$$

In a similar manner the synthesized pattern, computed at M field points, can be expressed as

$$g = [g_m] = \begin{bmatrix} g_1 \\ g_2 \\ \cdot \\ \cdot \\ \cdot \\ g_M \end{bmatrix} \quad . \tag{2}$$

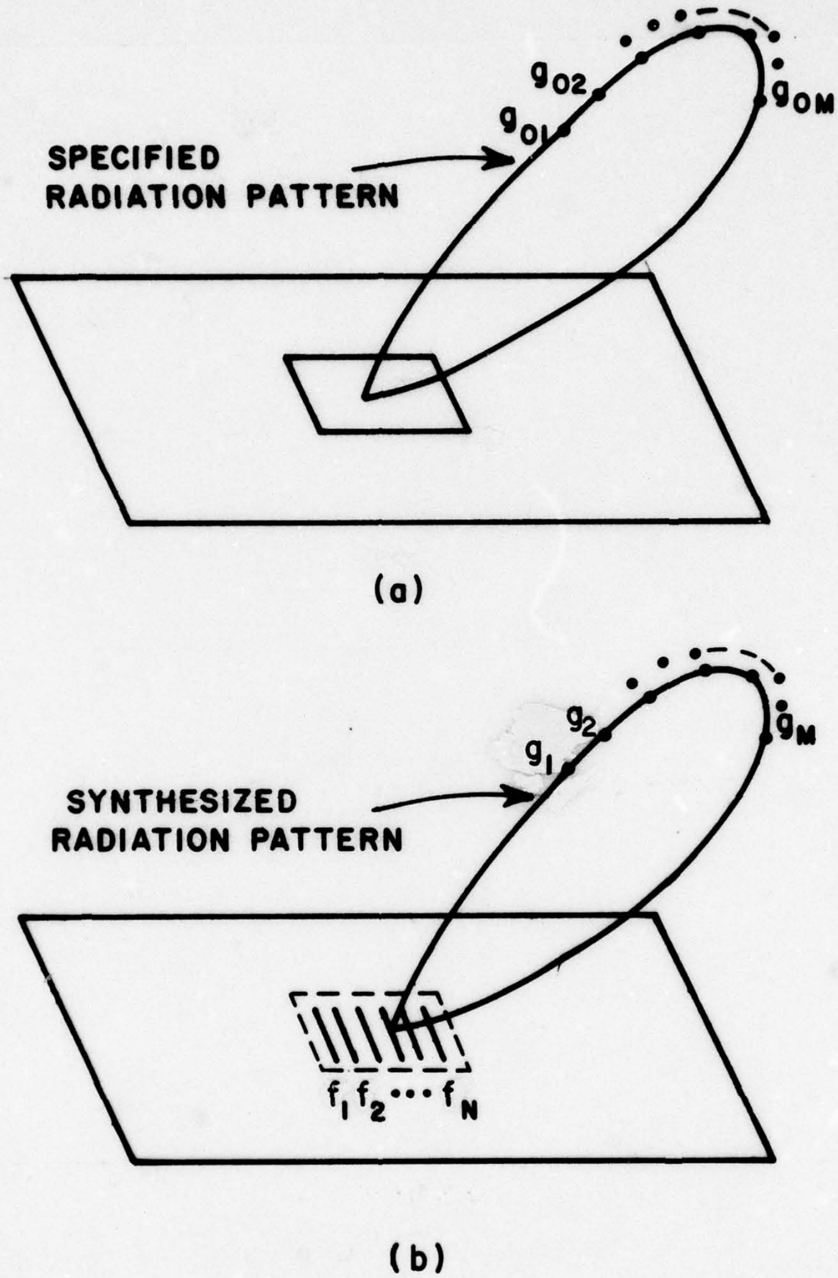

Figure 1. A typical antenna geometry and its analytical description.

a) Actual antenna geometry
b) Analytical model of the antenna

The source and resulting field are then formally related according to the relation

$$[T]f = g. \tag{3}$$

Here $[T]$ is an MxN matrix, expressed as

$$[T] = [T_{mn}] = \begin{bmatrix} T_{11} & T_{12} & \cdots & T_{1N} \\ T_{21} & & & \cdot \\ \cdot & & & \cdot \\ \cdot & & & \cdot \\ \cdot & & & \cdot \\ T_{M1} & \cdots & \cdots & T_{MN} \end{bmatrix} \tag{4}$$

where

T_{mn} = the field of the nth elemental source, evaluated at the mth field point location.

The synthesis problem can now be expressed by the approximate relation

$$[T]f \approx g_o \tag{5}$$

where g_o is the finite or infinite set of specified field values (Note that g in Equation (3) is the set of M synthesized field values, resulting from the N elemental sources). It may be noted that there are several ways to solve Equation (5) for the unknown set of sources $[f_n]$. For example, if the matrix $[T]$ is square and non singular Equation (5) can be inverted directed to yield the set of values $[f_n]$. In this case the field can be synthesized correctly at M pattern points, but no control of the pattern is obtained between these points. If M is less than N, the problem is underspecified (i.e., there are more unknowns than independent equations), and it is possible to obtain more than one set of $[f_n]$ which satisfy Equation (5). Finally, if M is greater than N, then an exact solution usually doesn't exist, but a unique least squares solution can be found. This latter solution case is usually the most common one encountered in practice and is, therefore, the one adopted in this study.

It can readily be shown (e.g., see Reference [1]) that the set of $[f_n]$ can be determined which minimizes the pattern error in the sense of obtaining the least mean square error when Equation (5) is solved according to the relation

$$[f_n] = \left\{[\tilde{T}][T]\right\}^{-1}[\tilde{T}]\ g_o, \tag{6}$$

where the tilda over the matrix indicates conjugate transpose. The mean squared pattern error resulting from the above solution is given by

$$\varepsilon = \sum_{m=1}^{M} \left| \sum_{n=1}^{N} f_n\, T_{mn} - h_m\, e^{j\beta_m} \right|^2 , \tag{7}$$

where the mth specified pattern value has been expressed as

$$g_{om} = h_m\, e^{j\beta_m} . \tag{8}$$

The error as expressed by Equation (7) assumes that the pattern is specified in both amplitude and phase (Equation (8)). As discussed in the Introduction, pattern phase data may not be available or, for other reasons, may not be specified. In this situation a solution to Equation (6) which minimizes the pattern error can still be obtained. Specifically, for any set of solutions $[f_n]$ the pattern error is minimized when the terms in Equation (7) are in phase. This requires that the phases, β_m, of each of the field values satisfy the relation

$$e^{j\beta_m} = \frac{\sum_{n=1}^{N} f_n\, T_{mn}}{\left| \sum_{n=1}^{N} f_n\, T_{mn} \right|} . \tag{9}$$

When pattern magnitude only data is specified (i.e., the h_m, in Equation (8)) an iteration process is used to find a set of β_m which satisfy Equation (9) (and which thereby yield a solution for the sources $[f_n]$ which minimize the pattern error ε according to Equation (7)). The steps in the basic iteration procedure, as given in Reference [1], are summarized as follows:

1. Assume starting values for the field point phases $\beta_1, \beta_2, \cdots \beta_M$.

2. Keep the β_m fixed and compute the elemental source values f_n which minimize the pattern error ε, using Equation (6).

3. Keep the f_n fixed and compute the β_m which minimize ε, using Equation (9).

4. Repeat steps 2 and 3 in iterative fashion until a small and stable value of ε is obtained.

Although numerical computations performed with this basic iteration procedure lead to a convergent solution for the elemental sources f_n, the rate of convergence has been found to be rather slow in some cases. In order to reduce the number of iterations required for convergence, a modified procedure was developed. Within a given iteration, the modified procedure makes incremental changes in both the computed f_n and the computed β_m (i.e., following steps 2 and 3, respectively, above), based upon the change in these values between successive iterations. The modified procedure is included in the computer code presented in Appendix A, and has been found to reduce the number of iterations required by about a factor of ten in most instances, compared to the basic procedure. Finally it should be noted that although the synthesis procedure discussed here generally yields satisfactory solutions, the solutions obtained are not unique. For example, depending upon the assumed starting values for the field point phases (i.e., step 1 in the iteration procedure) one could obtain somewhat different solutions for the sources f_n.

III. NUMERICAL IMPLEMENTATION OF THE PROCEDURE

This section contains a discussion of some of the specific details pertinent to practical application of the synthesis procedure. Examples are presented which demonstrate the techniques and are representative of results obtainable. For the present discussion it is assumed that the antenna is linearly polarized, and that its pattern is specified by measured principal plane pattern data. Also, the size and shape (e.g., rectangular) of the aperture are assumed to be known and, if the antenna aperture is flush-mounted in a finite ground plane, the dimensions of the ground plane are also assumed to be given.

With the antenna characteristics physically and electrically defined as indicated above, the first step in numerically implementing the synthesis procedure involves selection of appropriate values for M and N, which it may be recalled are the total number of specified field point values and the total number of elemental sources, respectively. In general, appropriate selection of the values for both M and N are directly related to the size of the antenna aperture. (That is, as the aperture size increases, the appropriate values for both M and N should be correspondingly increased.) As will be demonstrated shortly, adequate representation of the aperture distribution usually requires that the elemental sources be spaced on the order of $.25\lambda$ apart. With the size of the aperture known and the elemental source spacing selected as just indicated, a suitable value for the number of sources N can be chosen. As noted earlier the number M, of field point values selected, will generally be considerably larger (e.g., 3-20 times larger) than the number of elemental sources employed. In practice, the actual number of field point values selected involves making a tradeoff between desired accuracy and computational efficiency. On the one hand enough field point values should be selected from the given pattern data to describe the detailed structure of the pattern with reasonable accuracy. On the other hand, selection of a large number of field points increases computation time and may not yield a substantially better solution. In any event, an appropriate selection of field points (both in number and relative location) can usually be obtained by inspection from the given pattern data.

Having selected a list of field point values and an appropriate number of sources as described above, an analytical model of the radiating aperture is established to compute the elements of the matrix $[T_{mn}]$ associated with the fields of the elemental sources, as defined in Equation (4). For the examples to be presented, the elemental sources employed are magnetic line sources. A typical geometry depicting their placement within the known aperture configuration is depicted in Figure 2.

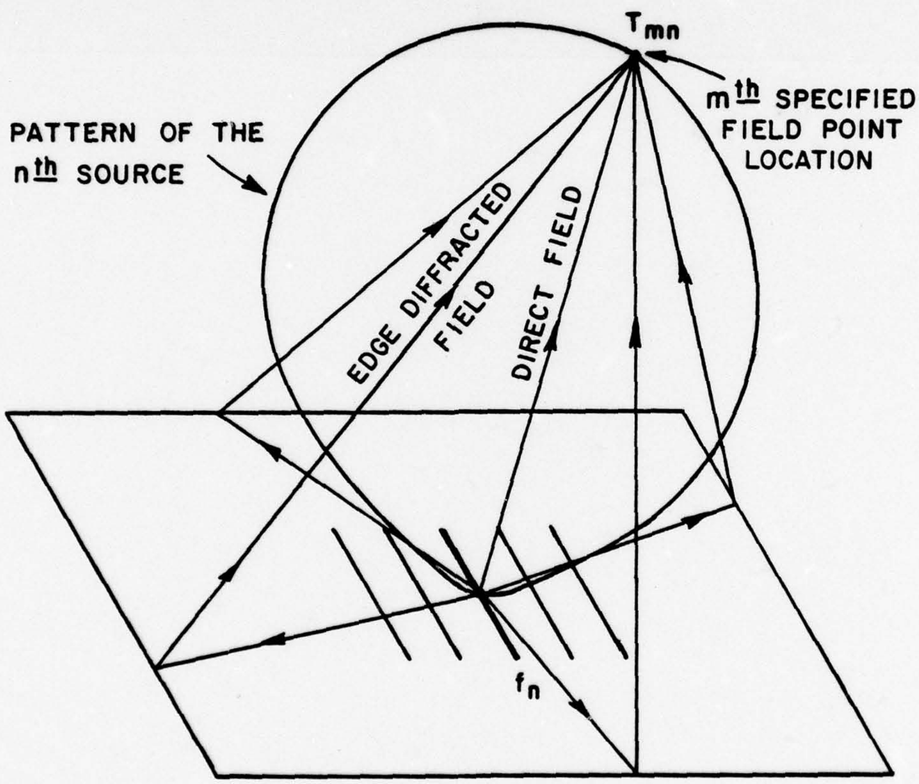

Figure 2. Geometry depicting computation of a matrix element T_{mn}. A matrix element is the computed value of the total field radiated by the nth elemental source f_n, evaluated at the mth specified location.

As may be recalled from the previous section each element of the matrix $[T_{mn}]$ is simply the computed value of the field of the nth elemental source evaluated at the mth selected field point location. Evaluation of the T_{mn} is straight-forward, and need be computed only once (assuming that the values are stored). If, as depicted in Figure 2, the aperture is mounted in a finite ground plane, the diffracted fields from the plate edges may be included in the computation by superposition with the direct field from each elemental source. When the effects of a finite ground plane are included in this manner selection of field point values will be most effective if all of the field values are chosen from the half-space directly illuminated by the aperture (i.e., the half-space on the antenna side of the ground plane, in Figure 2).

As a first typical example of the type of antenna which can be treated with the foregoing analysis, the antenna configuration depicted in Figure 3a was constructed. The measured E-plane radiation pattern (i.e., pattern plane is the x-z plane in Figure 3a) for this antenna is depicted in Figure 3b. Since the 1.33 inch width of the antenna aperture corresponds to about 1.25 wavelengths at the 11 GHz measurement frequency, six magnetic line sources were selected to model the aperture. The sources were uniformly spaced and oriented parallel to the y axis (see coordinate system of Figure 3a). For specified pattern data points, a set of 91 field values were selected from the measured pattern data of Figure 3b. In order to demonstrate how the iterative synthesis procedure converges to a final solution for the antenna of Figure 3, Figure 4 shows a sequence of patterns computed after 1, 10, 20, 40 and 80 iterations of the numerical synthesis procedure. The measured data points employed to obtain the computed solution are shown on each pattern, and the computed relative magnitude and phase of the six elemental sources (from which each pattern is computed) are listed adjacent to each of the respective patterns. Finally, the pattern errors obtained at each of the indicated stages of the solution are also shown. The desired information in the solution as depicted sequentially in Figure 4 is, of course, the list of complex source values obtained after solution convergence is achieved. Convergence of the solution is achieved when the list of source values obtained remains relatively constant (or alternatively, when the pattern error values reach a relatively stable minimum value). For the solution depicted in Figure 4, a convergent solution was obtained after about 40 iterations (Figure 4d). This can be seen by comparing the results obtained after 40 and 80 iterations (Figures 4d and 4e, respectively).

Although one might choose to gauge solution convergence visually by comparing the synthesized pattern with the specified measured data points, this is not always a reliable approach. Because of errors in the measured pattern data (or, equivalently, failure to include a minor feature of the physical problem in the analytical model), the synthesized pattern may exhibit an irreducible error in some region of the pattern,

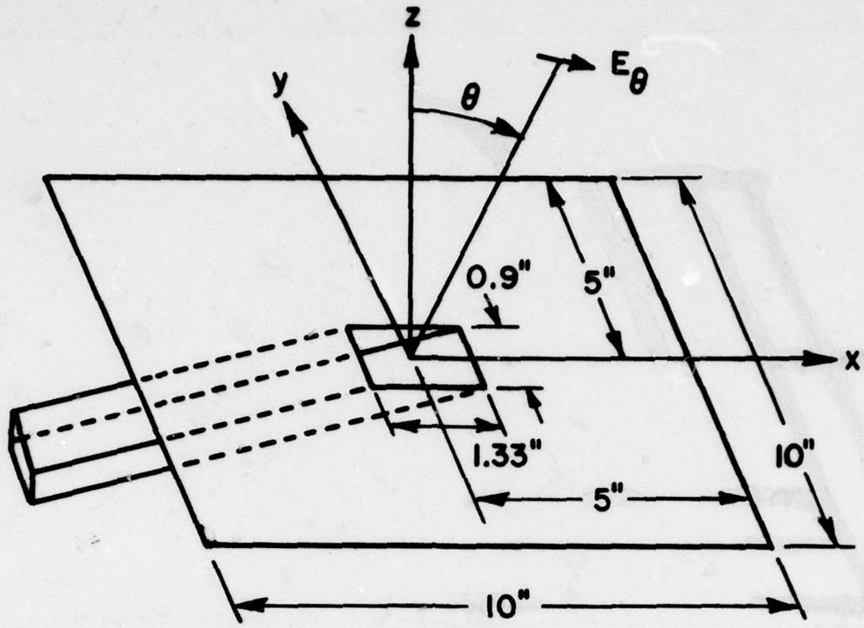

(a)

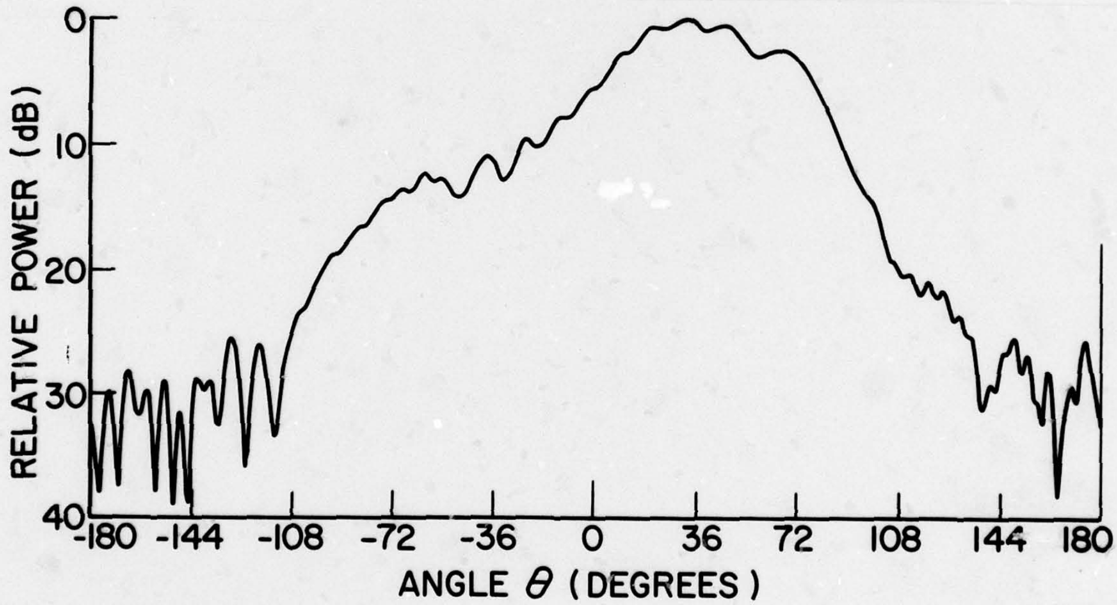

(b)

Figure 3. The first example antenna configuration and its measured pattern.

a) The antenna geometry
b) Its measured E-plane radiation pattern

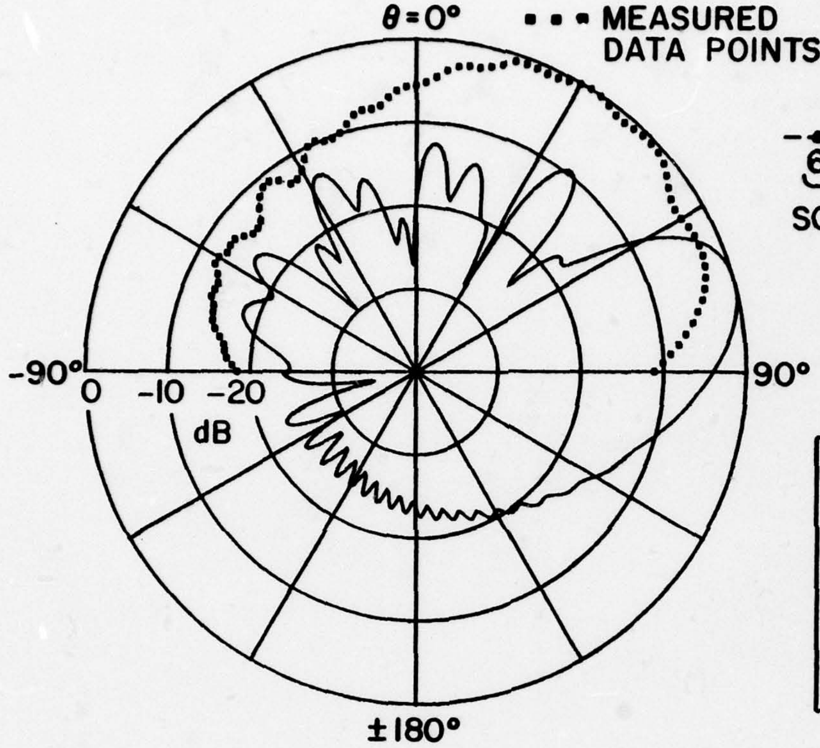

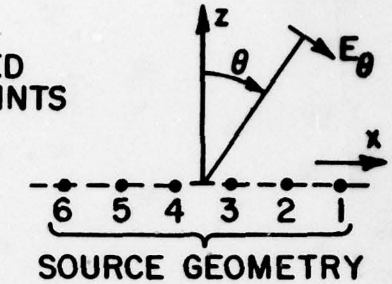

COMPUTED SOURCE VALUES

	MAG.	PHASE (DEG.)
1	0.184	21.91
2	0.604	-170.18
3	1.0	0.0
4	0.997	171.17
5	0.597	-17.18
6	0.179	154.95

PATTERN ERROR (E) = 0.649

(a) Solution obtained after 1 iteration

Figure 4. Sequential representation of computed source values, and corresponding radiation patterns, for the antenna of Figure 3. The results shown demonstrate, in sequence, the manner in which a convergent solution is obtained by use of the iterative synthesis procedure.

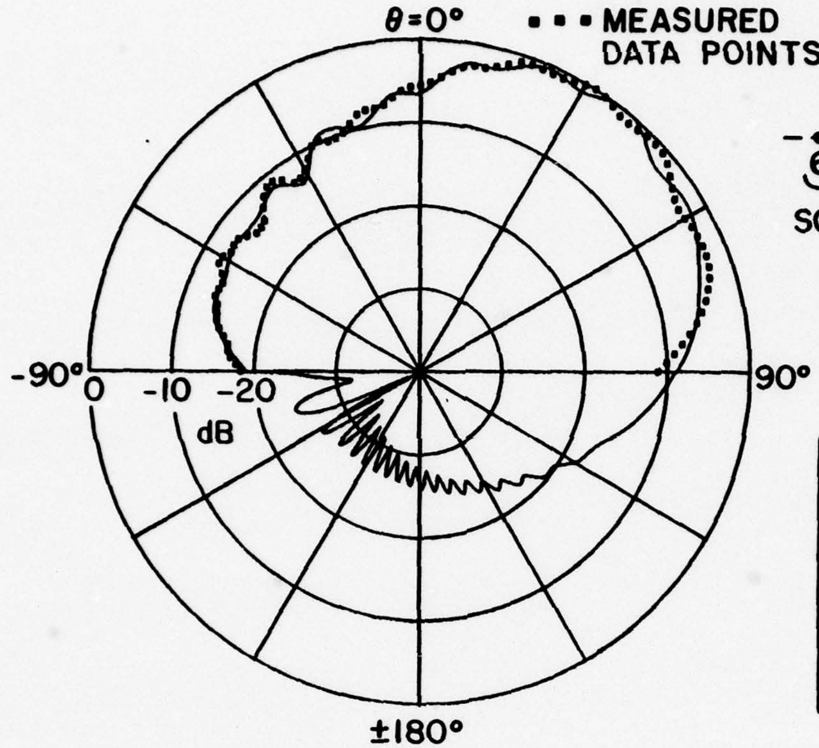

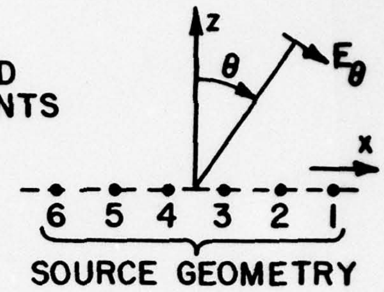

COMPUTED SOURCE VALUES

	MAG.	PHASE (DEG.)
1	0.346	14.16
2	0.783	-177.34
3	1.0	0.0
4	0.817	176.20
5	0.388	-6.85
6	0.091	173.62

PATTERN ERROR (E) = 0.00761

(b) Solution obtained after 10 iterations

Figure 4. (Continued)

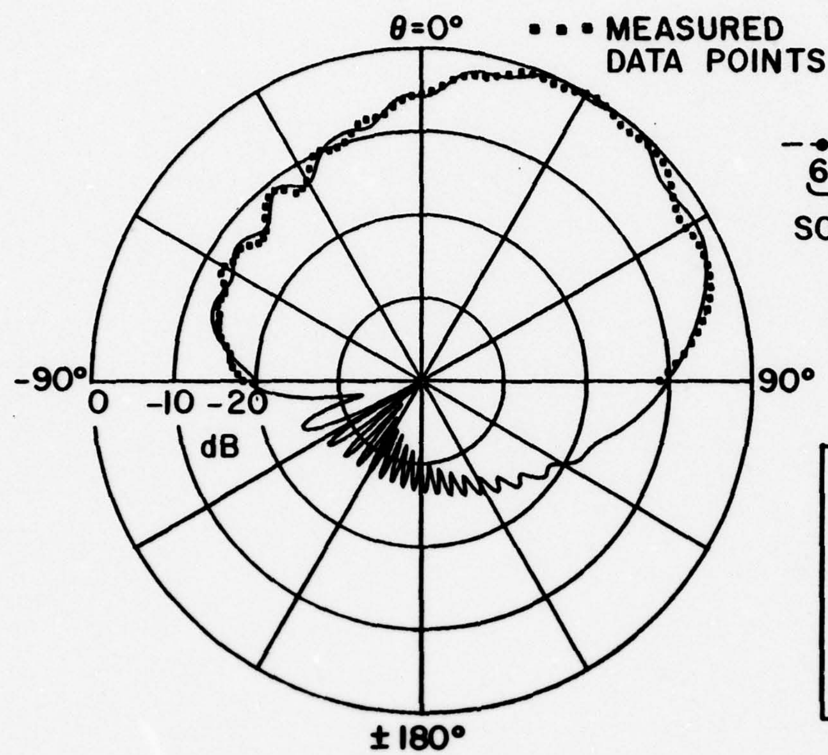

PATTERN ERROR (E) = 0.00566

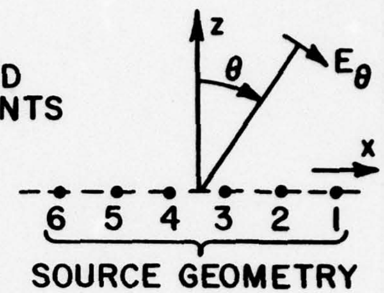

COMPUTED SOURCE VALUES

	MAG.	PHASE (DEG.)
1	0.462	8.09
2	0.873	177.44
3	1.0	0.0
4	0.749	179.20
5	0.310	19.45
6	0.069	-165.82

(c) Solution obtained after 20 iterations

Figure 4. (Continued)

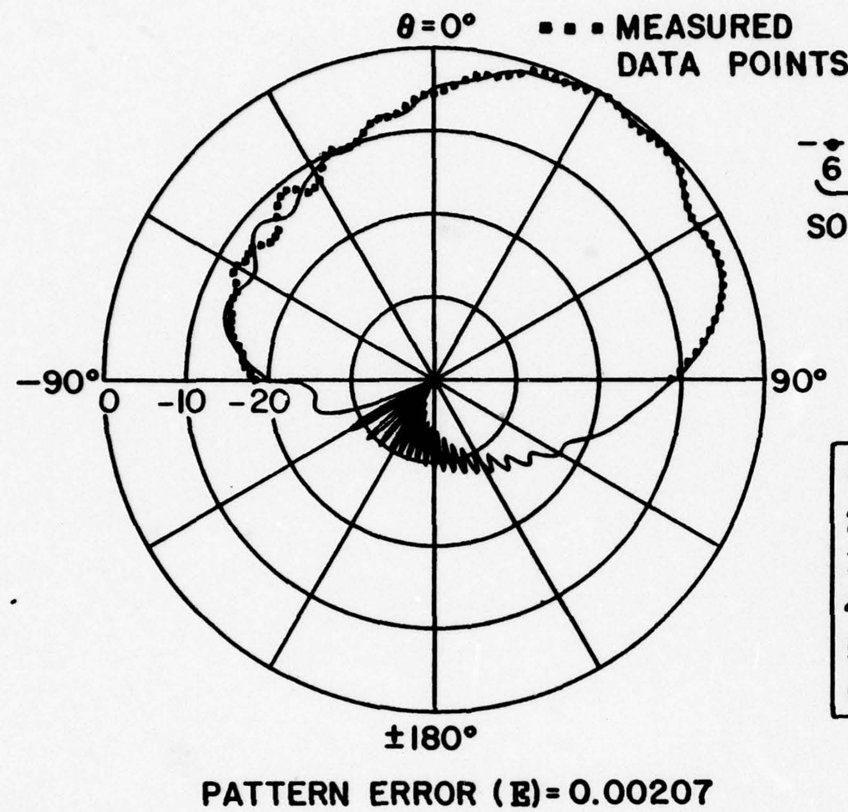

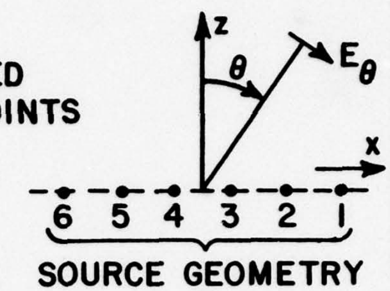

COMPUTED SOURCE VALUES

	MAG.	PHASE (DEG.)
1	0.413	4.18
2	0.734	178.64
3	1.0	0.0
4	0.817	168.73
5	0.338	−19.65
6	0.069	163.72

(d) Solution obtained after 40 iterations

Figure 4. (Continued)

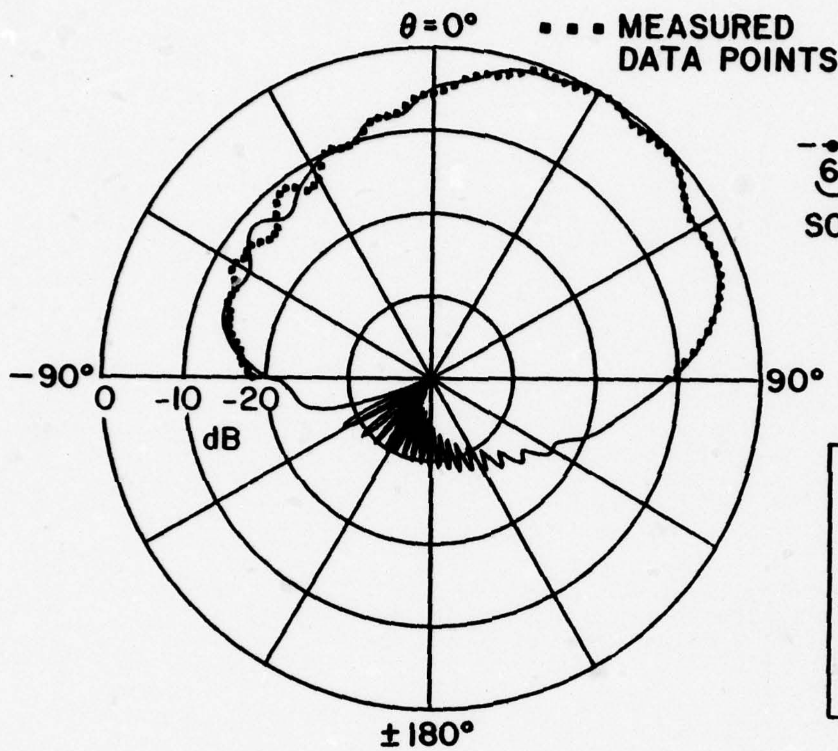

PATTERN ERROR (E)= 0.00201

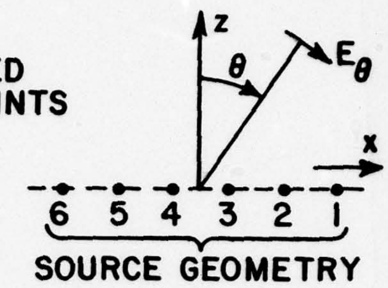

COMPUTED SOURCE VALUES

	MAG.	PHASE (DEG.)
1	0.373	2.92
2	0.727	178.44
3	1.0	0.0
4	0.835	171.87
5	0.385	−14.71
6	0.088	164.21

(e) Solution obtained after 80 iterations

Figure 4. (Continued)

even after a convergent solution has been attained. This situation is apparent in a portion of the computed patterns of Figures 4d or 4e. Since measurement errors tend to increase as the pattern levels decrease, it may be advantageous to specify fewer measured data points in the lower radiation level regions of the pattern. This technique is demonstrated in Figure 5, which shows the solution of Figure 4 recomputed using fewer measured data points (i.e., 65 data points were used instead of the original 91). In selecting the measured data points of Figure 5, the original data set was thinned by retaining only every other one of the original points in regions of the pattern with signal levels in the range between 10 and 15 dB below the peak pattern level, and retaining only every third data point in regions of the pattern with signal levels more than 15 dB down. It may be noted, by comparing the solution of Figure 5 with that of Figure 4d, that virtually the same solution is obtained when fewer data points are employed in this manner. In addition, the computation time was reduced substantially by use of fewer specified pattern data points.

As a second application of the synthesis procedure, the antenna geometry of Figure 6a was considered. This antenna was constructed and tested several years ago by Walter [2] as part of a study of endfire radiators. We have applied the synthesis procedure to an available measured pattern for this antenna as shown in Figure 6b. Although the antenna geometry of Figure 6a is similar in basic design to that just considered, it differs from the latter in two important respects. Specifically the aperture of the antenna in Figure 6a is roughly three times as large as that shown in Figure 3, and in addition, its aperture and waveguide feed were filled with dielectric. For the aperture of the antenna of Figure 6, 12 magnetic line sources were used to model its aperture distribution. The computed pattern obtained by applying the synthesis procedure is shown in Figure 7. The set of measured data points employed (as obtained from the measured pattern of Figure 6b) are shown on the pattern for comparison. The computed values of the 12 line sources from which the synthesized pattern was computed are also shown, as is the pattern error value obtained after solution convergence was attained (i.e., after 50 iterations, for the data shown in Figure 7).

The computed pattern of Figure 7, obtained by use of 12 sources to model the aperture, agrees very closely with the measured pattern from which it was synthesized (i.e., Figure 6b). In order to demonstrate how the quality of such solutions may degrade if too few sources are used to model the aperture distribution, the synthesis procedure was applied again to the same problem, but with only 7 sources employed to model the aperture distribution. The resulting solution is shown in Figure 8. The relatively poor agreement between the computed and measured patterns of Figure 8 and Figure 6b, respectively, is readily apparent, and is thought to be typical of the solution difficulties which may arise if too few sources are employed to model the aperture. As shown by the previously considered examples, this situation can be avoided by employing source spacings on the order of a quarter wavelength.

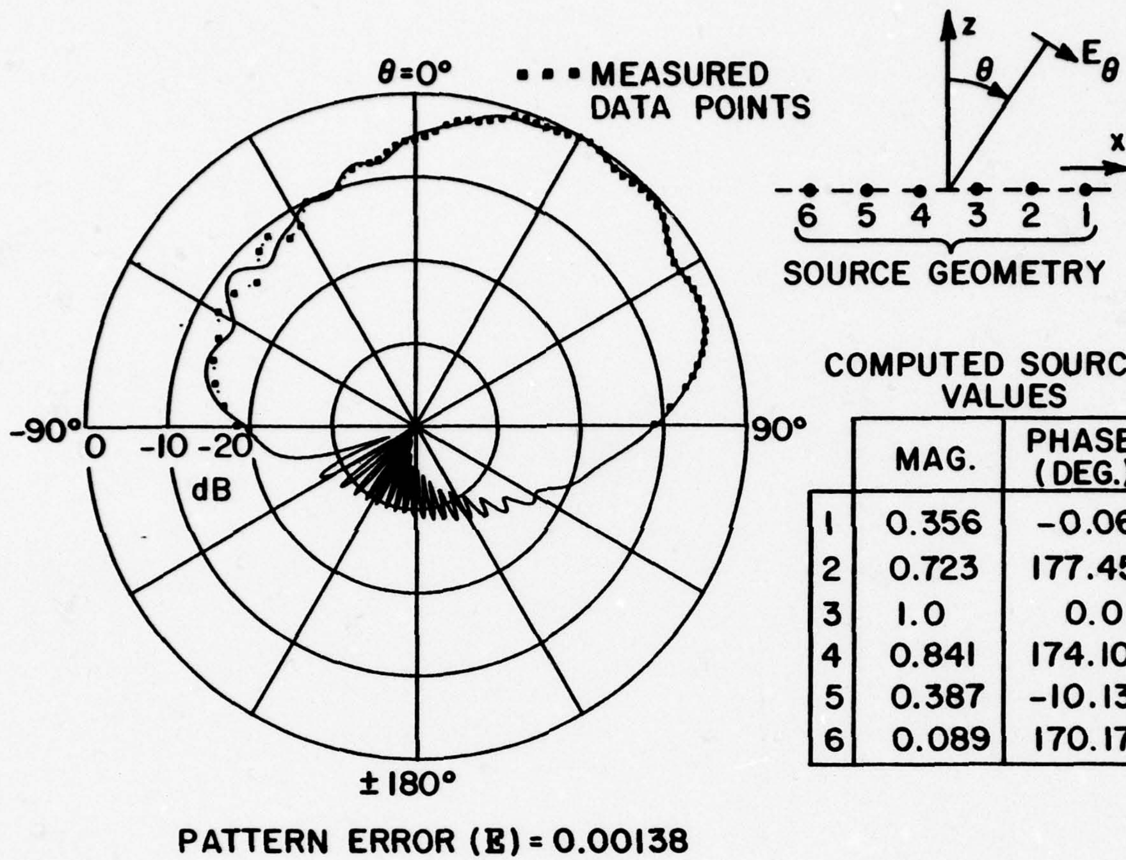

COMPUTED SOURCE VALUES

	MAG.	PHASE (DEG.)
1	0.356	-0.06
2	0.723	177.45
3	1.0	0.0
4	0.841	174.10
5	0.387	-10.13
6	0.089	170.17

Figure 5. Computed solution for the antenna of Figure 3, obtained by using fewer data points from the low signal level regions of the measured pattern. It may be noted that the solution obtained is virtually identical to the converged solutions of Figures 4d and 4e.

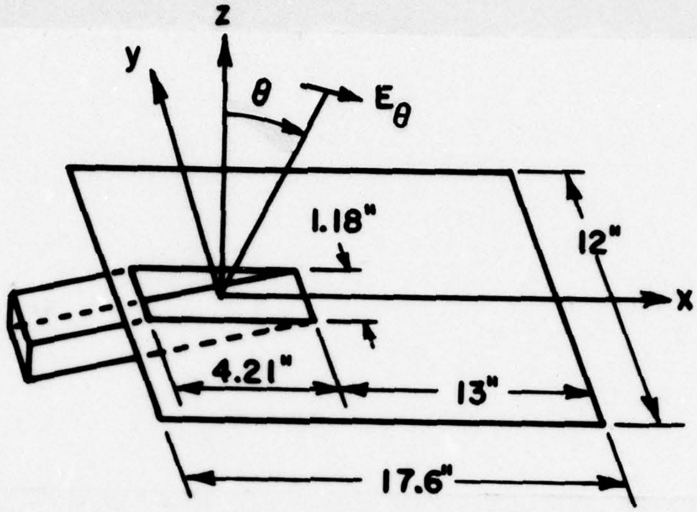

(a)

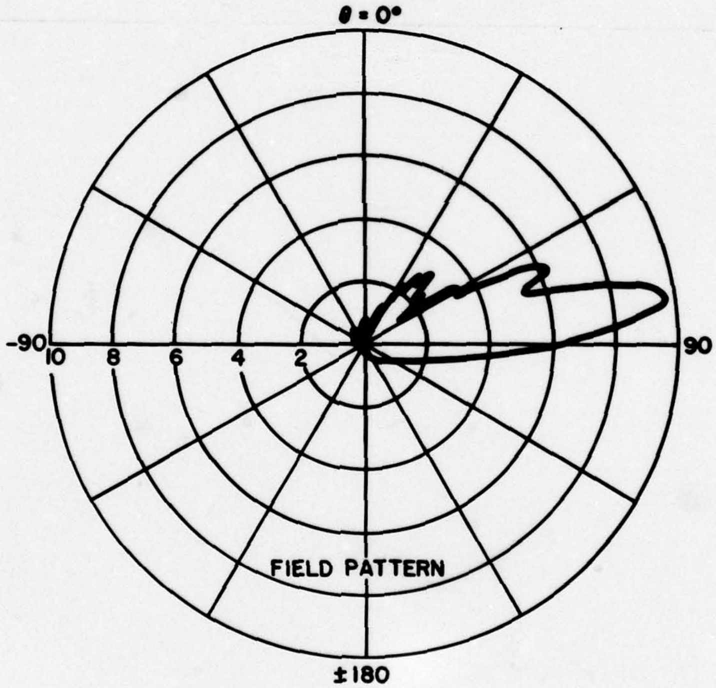

(b)

Figure 6. Second example antenna and its measured pattern.

a) Actual antenna geometry
b) Its measured E-plane pattern

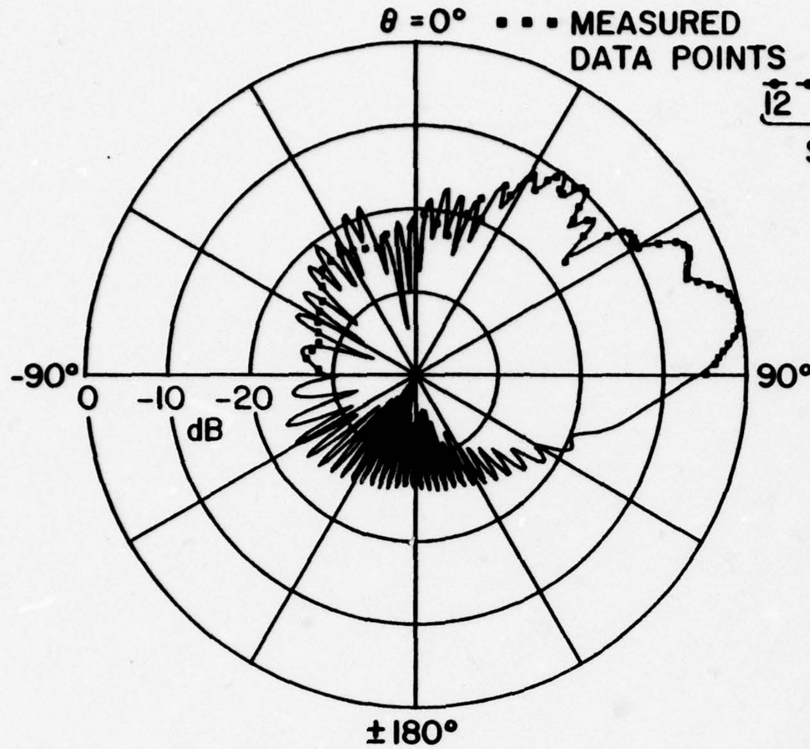

PATTERN ERROR (E) = 0.00101

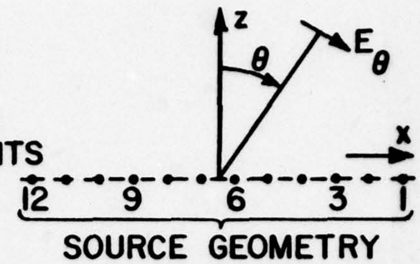

COMPUTED SOURCE VALUES

	MAG.	PHASE (DEG.)
1	0.023	27.99
2	0.104	-158.22
3	0.275	15.93
4	0.530	-168.40
5	0.806	7.63
6	0.991	-176.28
7	1.0	0.0
8	0.827	176.06
9	0.547	-8.04
10	0.277	168.11
11	0.099	-14.74
12	0.020	165.52

Figure 7. Computed source values and corresponding pattern for the antenna of Figure 6. As shown in the insert, 12 elemental line sources were used to model the antenna aperture.

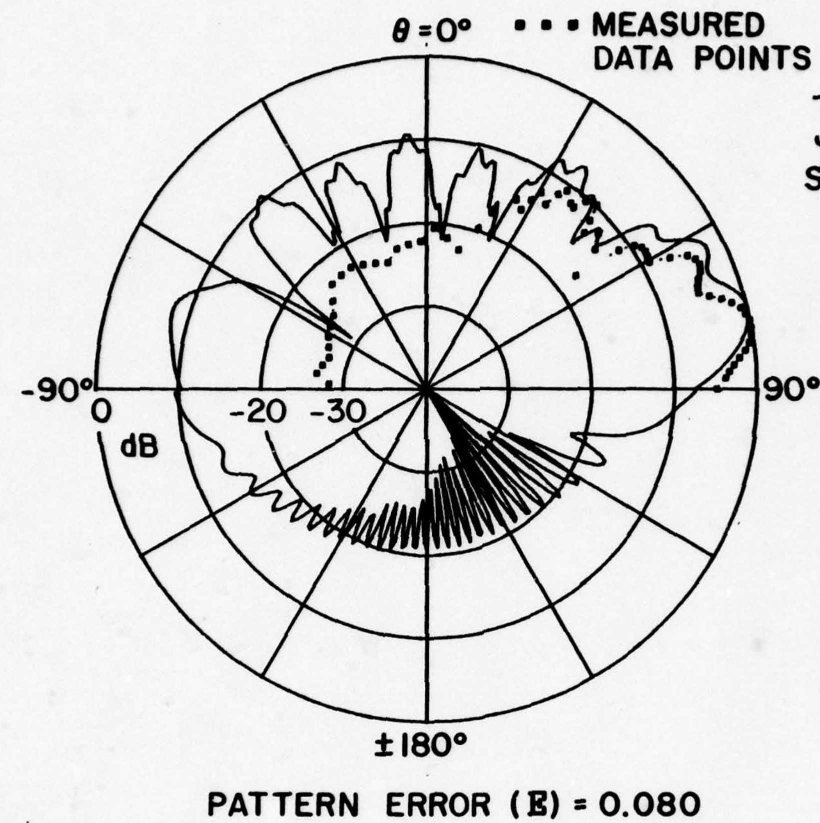

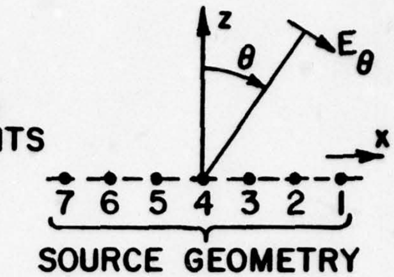

COMPUTED SOURCE VALUES

	MAG.	PHASE (DEG.)
1	0.639	7.40
2	0.384	-114.10
3	0.413	6.23
4	0.357	-113.03
5	0.575	48.48
6	0.745	-151.41
7	1.0	0.0

Figure 8. Computed source values and corresponding radiation pattern for the antenna of Figure 6, using only 7 elemental sources to model the aperture. Comparison of the computed pattern shown with that of Figure 7 reveals the solution degradation resulting from use of too few sources to model the aperture.

The example solutions presented thus far have demonstrated that the synthesis procedure provides a useful method for computing the aperture distribution of an antenna, given its measured radiation pattern and basic physical dimensions. As discussed in the Introduction, the ultimate intended purpose of the procedure is to be able to employ an antenna's computed aperture distribution to predict the same antenna's radiation pattern performance in a different structural environment (e.g., when the antenna is mounted on an aircraft fuselage). As a demonstration of extending the analytical solution in this manner, the antenna geometry of Figure 3 was modified for further testing. To simulate its introduction into a new structural environment, an adjustable ground plane was added to the original antenna geometry, as depicted in Figure 9. Then,

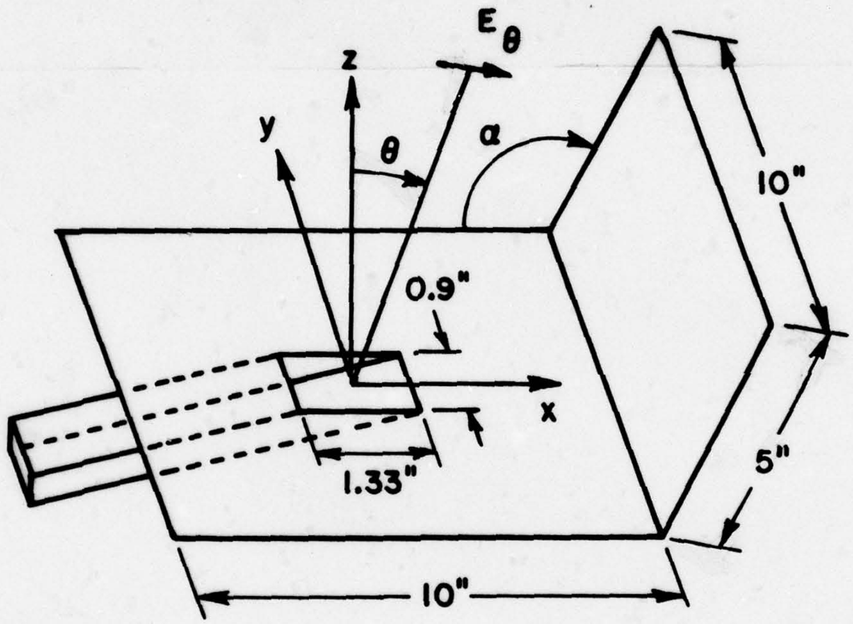

Figure 9. Modified version of the antenna geometry of Figure 3. Measured and computed patterns pertaining to this geometry are presented in Figure 10.

using the computed aperture distribution for the original geometry (as listed in Figure 4d) together with a two-plate diffraction theory model of the modified antenna's ground plane structure, radiation patterns were computed for the new geometry, and compared with pattern measurements of the new geometry. The computed and measured patterns obtained are compared in Figure 10, for several selected positions of the adjustable ground plane. It may be noted that although the computed and measured patterns are not in perfect agreement, the extent of agreement is thought to be very good, especially in view of the fact that the computed solution originated from a different measured pattern.

A basic question of validity in applying the above technique hinges on the validity of the assumption that the antenna's aperture distribution remains essentially invariant when the antenna is introduced into a new structural environment. The comparison between computed and measured patterns presented in Figure 10 provides strong evidence that this assumption is valid for the modified geometry considered. As a more direct check of the invariance of the aperture distribution, the synthesis procedure was applied directly to both the original antenna geometry of Figure 3 and the modified geometry of Figure 10d (i.e., the case of a 5" planar extension added to the ground plane of the original antenna). The resulting computed aperture distributions, obtained for each geometry after 50, 60, 70, and 80 iterations of the respective solutions, are listed in Table I. Both solutions have essentially converged after 40 iterations, and the indicated changes in either of the respective solutions after 50, 60, 70, or 80 iterations are simply minor oscillatory adjustments inherent in the solution, as it progresses. By comparing the aperture distributions computed for the respective antenna geometries after a given number of iterations (e.g., after 80 iterations of each solution), it may be seen that the distributions computed for the respective geometries are in very close agreement. In fact, since the extent of agreement between solutions is roughly commensurate with that obtained within each solution as the number of solution iterations changes, the distributions computed for the two respective geometries could be viewed as being virtually identical.

IV. CONCLUSIONS

A synthesis procedure is presented which provides an efficient means for numerically computing the aperture distribution of an antenna, based on its specified radiation pattern characteristics. The viewpoint adopted here differs substantially from that of the traditional synthesis problem, however, in that the specified pattern is considered to consist of measured pattern data obtained from an existing well-defined antenna geometry. As applied, the solution of importance is the computed aperture distribution for the given antenna. Subsequently, the computed aperture distribution may be used to predict (i.e., compute) the radiation pattern performance of the given antenna in a different structural environment as, for example, when mounted on an aircraft. The anticipated utility of such a procedure when used in conjunction with available computer-aided design techniques, provided the primary motivation for this investigation.

The methods presented are applicable to antennas having either continuous or discrete apertures mounted in a finite or infinite ground plane. Since the given pattern data are assumed to be specified in

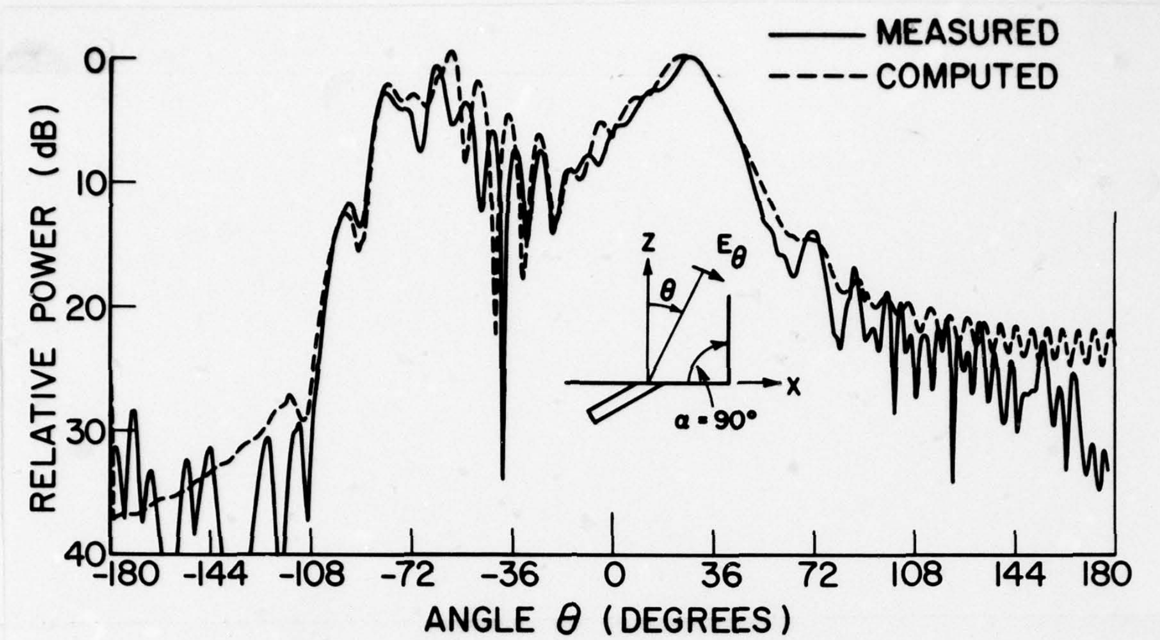

(a) 90° angle between plates

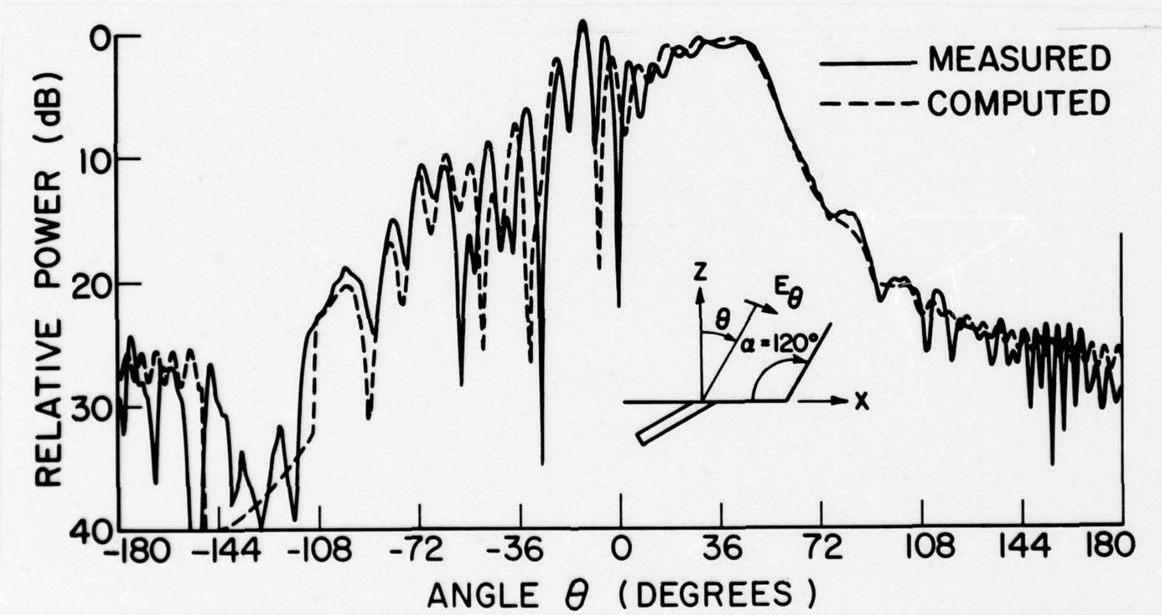

(b) 120° angle between plates

Figure 10. A specific example of how the results of the synthesis procedure can be used for pattern prediction. The computed patterns shown are for the modified antenna of Figure 9, and were obtained by using the computed source distribution for the unmodified antenna of Figure 3 (i.e., the source values of Figure 4d). A two-plate model is used to simulate the structure. The measured patterns shown were obtained directly from the antenna geometry depicted in Figure 9.

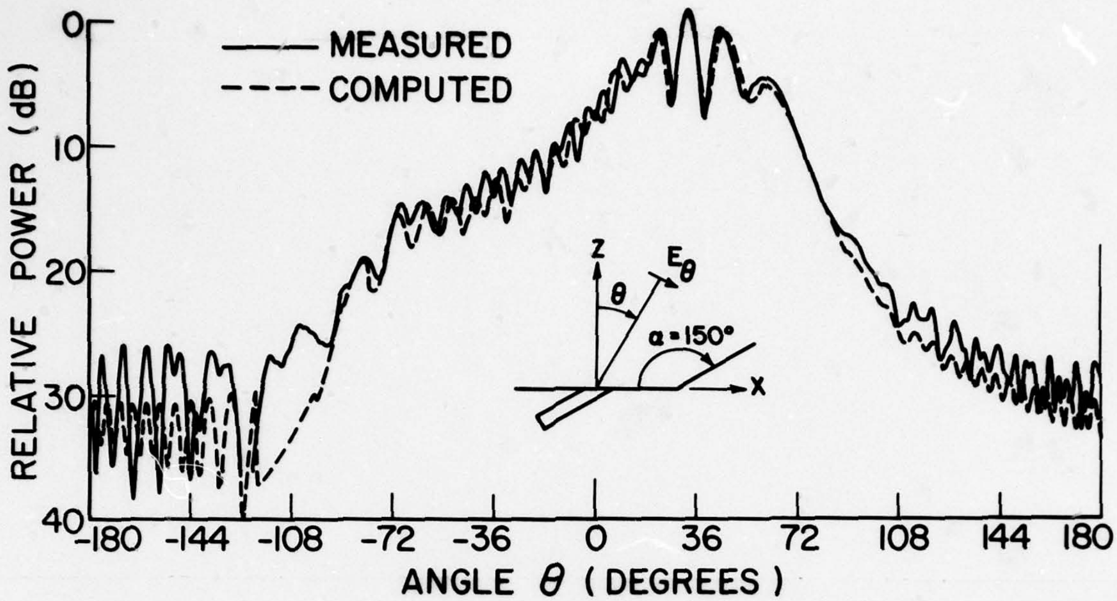

(c) 150° angle between plates

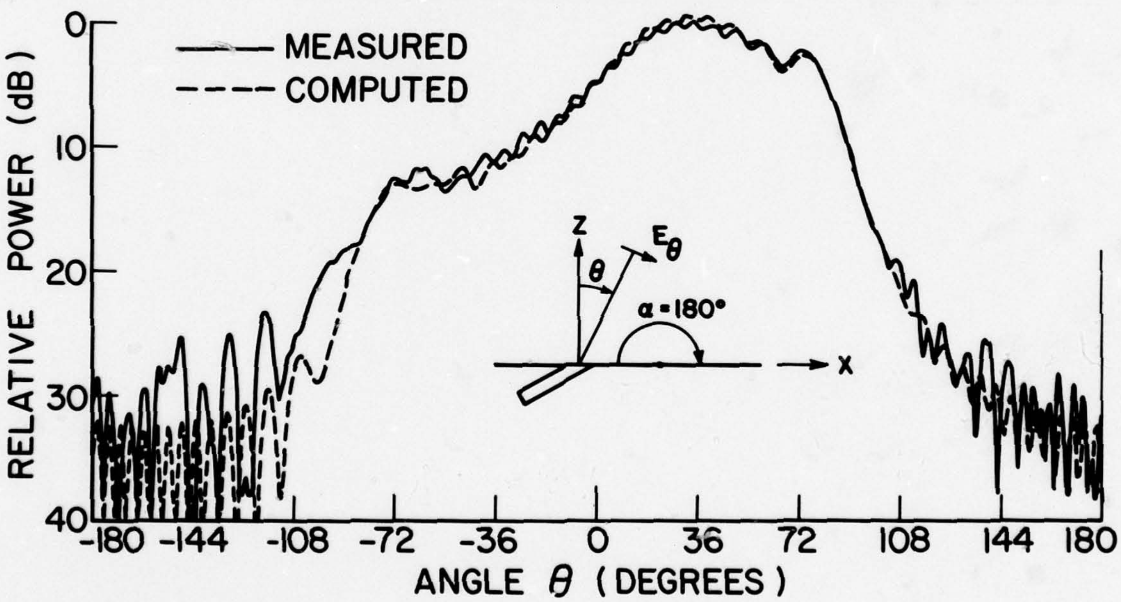

(d) 180° angle between plates

Figure 10 (Continued).

TABLE I

Source Values Obtained After 50, 60, 70 and 80 Iterations, For The Antennas of Figure 3, and of Figure 9 With α=180°.

	Antenna of Figure 3			Antenna of Figure 9 (α=180°)	
	Mag.	Phase		Mag.	Phase
50			50		
1	.388627904794D+00	.382212322977D+01	1	.489492586841D+00	-.176149066536D+01
2	.730249013136D+00	.178678596250D+03	2	.702892278608D+00	.174737836122D+03
3	.100000000000D+01	.141793267545D-09	3	.999999999992D+00	-.190948144463D-09
4	.835028244244D+00	.170492265984D+03	4	.808195797446D+00	.167426375928D+03
5	.368704982496D+00	-.170214836377D+02	5	.329889441933D+00	-.175829854662D+02
6	.813250070177D-01	.162881317026D+03	6	.782458433318D-01	.169507075097D+03
60			60		
1	.365276380509D+00	.248982463037D+01	1	.470113812692D+00	-.267972251978D+01
2	.725112087944D+00	.178320273274D+03	2	.710666320079D+00	.174324989284D+03
3	.999999999996D+00	.298356427429D-10	3	.999999999996D+00	-.162943999411D-09
4	.847761757613D+00	.172533966009D+03	4	.822065104439D+00	.169885571157D+03
5	.392540106731D+00	-.136072393377D+02	5	.355825154056D+00	-.139887918113D+02
6	.912408204594D-01	.164982620839D+03	6	.875774103569D-01	.170448106684D+03
70			70		
1	.369004739892D+00	.269158449045D+01	1	.434459979571D+00	-.341828218485D+01
2	.726046531275D+00	.178375236869D+03	2	.720024995967D+00	.174555393344D+03
3	.100000000000D+01	.613938651910D-10	3	.999999999996D+00	.130071599699D-09
4	.845771570609D+00	.172217243184D+03	4	.834344063812D+00	.172715865444D+03
5	.388955385511D+00	-.141372255284D+02	5	.381903486822D+00	-.104317680796D+02
6	.897939699398D-01	.164603230684D+03	6	.954741639943D-01	.171394075985D+03
80			80		
1	.372971518960D+00	.291893643184D+01	1	.438750039120D+00	-.335774436434D+01
2	.726983317235D+00	.178437902643D+03	2	.719305298589D+00	.174515521652D+03
3	.999999999996D+00	.948933542454D-10	3	.999999999996D+00	.531838524937D-09
4	.843669170731D+00	.171872851405D+03	4	.832891015132D+00	.172416297773D+03
5	.385077410444D+00	-.147142838639D+02	5	.379042367316D+00	-.108023516436D+02
6	.882051481926D-01	.164207582202D+03	6	.946259687548D-01	.171266729878D+03

magnitude only, a numerical iteration process is required to evolve the unspecified phase information. In cases where both pattern magnitude and phase data are available, the solution for the desired aperture distribution may be obtained directly without using the iteration process. In addition to principal plane (e.g., E- and H-plane) pattern data, application of the synthesis procedure requires that the physical dimensions of the antenna aperture and the dimensions of the ground plane in which it is mounted (if any), be given. For antennas mounted in finite ground planes, the Geometrical Theory of Diffraction (GTD) is used to account for the effects of the ground plane edges. The antennas specifically considered in this investigation were composed of rectangular apertures, flush mounted in planar rectangular ground planes. For the apertures and pattern planes considered, the aperture distributions could be treated as one-dimensional. The basic methods presented are more generally applicable, however, and could be extended to treat non-planar apertures of arbitrary shape, which are flush mounted in curved surfaces.

During the course of the investigation the synthesis procedure was applied to several specific antenna geometries. The solutions obtained, as presented in Section III, serve to demonstrate the capabilities of the procedure. They also serve to point out some specific techniques which were found to be helpful in successfully implementing the procedure. It was found, for example, that the discrete sources employed to model the aperture distribution should be spaced about a quarter wavelength apart. As demonstrated by one of the examples, use of larger source spacings (e.g., spacings of $\lambda/2$) may result in relatively large errors in the synthesized pattern (indicating use of an inadequate aperture representation). Additional helpful techniques, relating to the most appropriate selection of data points from a given antenna pattern, were also deduced from the antenna geometries considered. When the antenna aperture is mounted in a finite ground plane, it was found that the most efficient selection of data points is obtained when all of the points are chosen from the illuminated half of the radiation sphere (i.e., from the aperture side of the ground plane). The reason for this is that the diffracted fields on the shadow-side of the ground plane (i.e., the total fields in this region) are only indirectly related to the aperture fields (through the field incident on the edge) and these fields are adequately represented by their inclusion in the illuminated half-space fields.

Aside from the data selection consideration just noted, one has a considerable degree of latitude in selecting both the number and relative location of pattern data points. When, as assumed here, the pattern data points are selected from a measured pattern, it may be helpful to select fewer data points from the low signal level regions of the pattern. This technique, which was demonstrated in the previous section, simply acknowledges the fact that errors in measured signal levels tend to be larger in the low level regions of the pattern. Choice of fewer inaccurate data values often yields as accurate a solution as can be obtained, with an expenditure of considerably less computation time. Finally, it has been observed that solution difficulties may result if the true angular orientation of the measured pattern data is not accurately specified. Specifically, if the angular orientation of the pattern data is incorrectly specified by even a small amount (e.g., 1 or 2 degrees), solutions were found to converge rapidly, but the resulting synthesized pattern typically exhibited a relatively large pattern error. It was found that this difficulty could be overcome, however, by rotating the entire data set by a small amount, and repeating the solution until the orientation yielding the smallest pattern error is determined. This can only be done for small angular error in the alignment of the ground plane. Consequently, one should attempt to obtain the best possible set of measurements for the antenna under consideration. It is obvious that one can not start with patterns with large measurement errors and hope to synthesize an error-free aperture distribution.

REFERENCES

[1] J. R. Mautz and R. F. Harrington, "Computational Methods for Antenna Pattern Synthesis," IEEE Trans. on Antennas and Propagation, Vol. AP-23, No. 4, July 1975, pp. 507-512.

[2] C. H. Walter, "End-Fire Slot Antennas," Report 486-12, 15 September 1953, The Ohio State University ElectroScience Laboratory (former Antenna Laboratory), Department of Electrical Engineering; prepared under Contract AF18(600)-85, for Air Research and Development Command, Wright Air Development Center, Wright-Patterson Air Force Base, Ohio. (AD 20000)

APPENDIX A

This appendix contains a brief, user oriented description and statement listing of the computer program developed as a part of the investigation. The program presented was used to obtain the computed results presented in Section III of the text. As presented, the program is written for use on an interactive system permitting teletype input and output. Provision is also included for visual cathode ray tube (CRT) display of the computed patterns, generated at specified intervals as the iterative solution progresses. Programming statements associated with these capabilities and other minor provisions which may not be conveniently implemented on other facilities, are noted with asterisks in the program listing. Comment statements (i.e., statements preceded by C!!!) are distributed throughout the program to describe the analytical function of various statement sequences.

As an aid in discussing the program, its major sections are depicted in block form in Table II. A brief description of the major functions performed within each of the letter-designated blocks is given as follows:

A - This block of statements (lines 21-52) inputs the antenna geometry, the integer number of sources (NS) chosen to model the aperture, the integer number (ITMX) of iterations desired, and the list of data values selected from the antenna's measured pattern. The antenna geometry is specified by inputting the dimensions SMIN, SMAX, and W, expressed in wavelengths. Definition of these quantities is depicted in Figure 11.

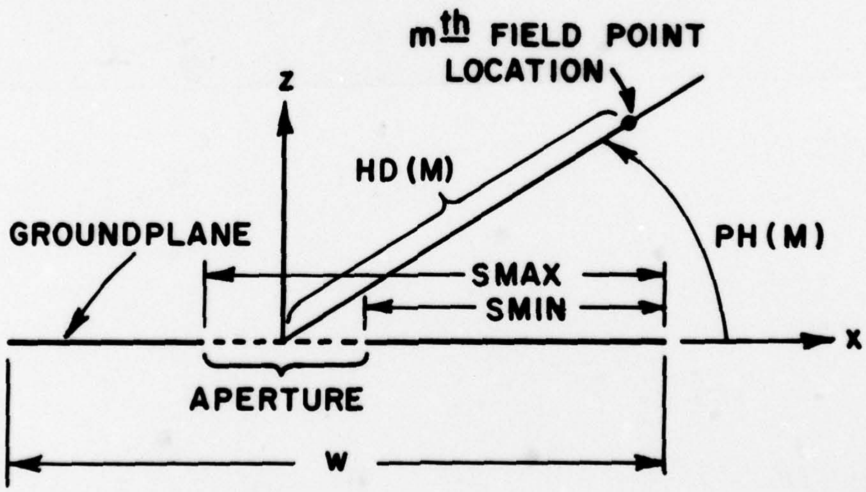

Figure 11. Geometry defining various antenna and pattern parameters used in the computer code.

TABLE II

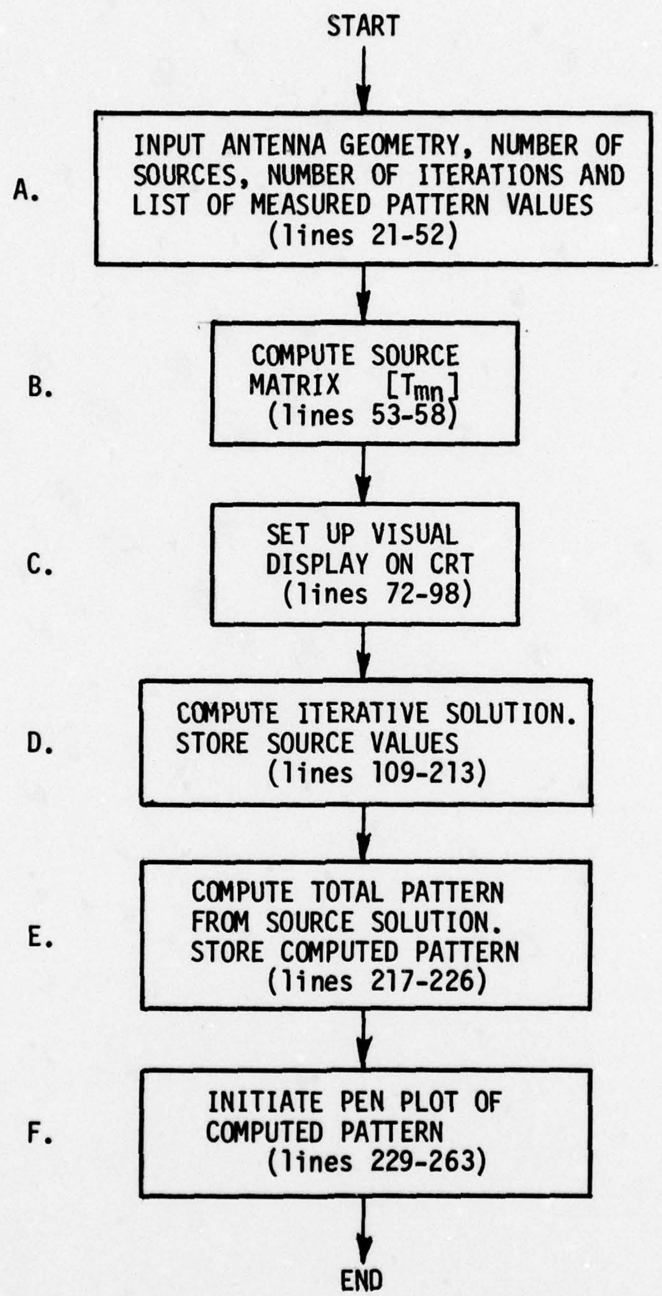
START
A.
INPUT ANTENNA GEOMETRY, NUMBER OF SOURCES, NUMBER OF ITERATIONS AND LIST OF MEASURED PATTERN VALUES
(lines 21-52)
B.
COMPUTE SOURCE MATRIX $[T_{mn}]$
(lines 53-58)
C.
SET UP VISUAL DISPLAY ON CRT
(lines 72-98)
D.
COMPUTE ITERATIVE SOLUTION. STORE SOURCE VALUES
(lines 109-213)
E.
COMPUTE TOTAL PATTERN FROM SOURCE SOLUTION. STORE COMPUTED PATTERN
(lines 217-226)
F.
INITIATE PEN PLOT OF COMPUTED PATTERN
(lines 229-263)
END

The pattern data values are defined by integer number (M), angle PH(M), and magnitude HD(M), as depicted in Figure 11. This data is read in free-format, from a separate file. The specific list of pattern data values used in the example of Figure 4 (Section III) is shown in Table III. Note that the first number to be read is the total integer number of data values contained in the list.

B - This group of statements (lines 53-58) computes the individual elements of the matrix $[T_{mn}]$, by making repeated calls to the function subroutine HPLN. This subroutine computes the total field (including diffraction from ground plane edges) of each elemental source at each field point location, and is listed following the main program.

C - This sequence of statements (lines 72-98) sets up a CRT display, consisting of a polar grid and plot of the selected measured data points. Later, in the iteration loop, a plot of the computed pattern is added to the display for the purpose of visual inspection of solution progress. The pattern is recomputed for display purposes at intervals specified by the integer variable NPLTMX (read in statement 98). A value of 5 for NPLTMX, for example, would result in a visual display update of the computed pattern after every 5th iteration. (If desired, this entire section may be bypassed or deleted, except for specification of a value for NPLTMX, which is used elsewhere in the program to write updated lists of the computed source values.)

D - This group of statements (lines 109-213) iteratively recomputes the solution, until a convergent result is obtained. The source and pattern error values computed after each iteration are written (the error values are written as teletype output) at intervals specified by NPLTMX. The computed pattern is also generated and displayed on the CRT at the same specified interval, as discussed above. If a visual display cannot be used, statements 160-172 should be bypassed or deleted.

E - This block of statements (lines 217-226) recomputes the total pattern after completion or termination of the iteration loop. The computed pattern values are stored in a binary file (named SYNSIS) for later use.

F - This group of statements (lines 229-263) initiates an optional polar pen plot of the final computed pattern. The measured pattern data points used as input in the procedure are also plotted on the same grid, for comparison with the computed pattern. The plots presented in Section III (e.g., see Figure 4) were obtained by using this plot section. This group of statements may be bypassed or deleted, if desired.

The above summary completes the discussion of the main synthesis program, which extends from statements 1-265 in the accompanying program listing. Several subroutines used in the main program are also included in the listing shown. Subroutines GRID and POLPLT are used in the various plot sections of the main program. The complex function subroutine HPLN is used to compute the source fields in the main program. Finally, subroutines DI and FRNELS are diffraction coefficient and fresnel integral subprograms required by the source subroutine HPLN. Two standard routines used by the program are not listed. One of these is the subroutine PLOT, which is a standard CALCOMP plot routine. The other subprogram not specifically listed is subroutine CGELG. This is a standard IBM program for solving simultaneous equations, which was modified slightly to treat complex arithmetic.

TABLE III

LIST OF MEASURED PATTERN DATA VALUES USED AS COMPUTER CODE
INPUT TO OBTAIN THE COMPUTED SOLUTIONS OF FIGURE 4

```
91
0.,-13.3
2.,-12.25
4.,-11.25
6.,-10.15
8.,-9.15
10.,-8.1
12.,-7.3
14.,-6.45
16.,-5.85
18.,-5.3
20.,-4.95
22.,-4.75
24.,-4.7
26.,-4.75
28.,-4.9
30.,-5.15
32.,-5.25
34.,-5.
36.,-4.45
38.,-3.8
40.,-3.15
42.,-2.75
44.,-2.65
46.,-2.7
48.,-2.9
50.,-3.05
52.,-3.
54.,-2.6
56.,-2.25
58.,-2.1
60.,-2.25
62.,-2.65
64.,-2.9
66.,-3.
68.,-2.88
70.,-2.85
72.,-3.
74.,-3.75
76.,-4.35
78.,-4.8
80.,-4.85
82.,-5.15
84.,-5.8
86.,-6.6
88.,-7.3
90.,-7.7
92.,-7.85
94.,-8.3
96.,-9.
98.,-9.8
100.,-10.
102.,-10.
104.,-10.3
106.,-11.2
108.,-12.
110.,-12.3
112.,-12.3
114.,-11.8
116.,-12.05
118.,-13.2
120.,-14.3
122.,-14.85
124.,-14.9
126.,-13.75
128.,-13.15
130.,-13.25
132.,-13.85
134.,-14.8
136.,-16.
138.,-16.3
140.,-16.28
142.,-15.65
144.,-15.
146.,-15.
148.,-15.15
150.,-14.6
152.,-14.6
154.,-15.5
156.,-16.
158.,-15.85
160.,-15.8
162.,-16.4
164.,-16.6
166.,-16.8
168.,-17.3
170.,-18.05
172.,-18.7
174.,-18.8
176.,-19.15
178.,-19.85
180.,-20.5
```

```
      OPTIONS DP
      OPTIONS 32K
      INCLUDE CGELGB,3390M;FLSBS,404C
      COMPLEX HS(120,40),TS,HITM(120),F(40),T(40,40)
     2,C(1600),HIT(361),HPLN,CJ,FF(40),HLAST(120)
      COMPLEX TOP,FAC
      DIMENSION IFILE(2),IUSER(2),PH(120),HD(120),
     2PHAR(120),IBUF(512)
      LOGICAL LOG,LVISD,LDB,LSOR,LPHASE
      COMMON/CONST/TOP
      COMMON/STORE/T,C,HS
      COMMON/PLAT/W,LSOR
      EXTERNAL CRTPLT,PLOT
      LSOR=.FALSE.
      PI=3.14159265
      TPI=2.*PI
      DPR=180./PI
      RPD=1./DPR
      CJ=(0.,1.)
      TOP=-CEXP(-CJ*0.25*PI)
      WRITE(8,1)
1     FORMAT(' MIN AND MAX DISTANCE OF APERTURE FROM EDGE=? ')
      READ(8,-) SMIN, SMAX
      WRITE(8,6)
6     FORMAT(' PLATE WIDTH IN WAVELENGTHS=? ')
      READ(8,-) W
      WRITE(8,2)
2     FORMAT(' NUMBER OF SOURCES TO SIMULATE APERTURE=? ')
      READ(8,-) NS
      CALL ESC($9898)
      WRITE(8,30)
30    FORMAT(' NUMBER OF ITERATIONS DESIRED=? ')
      READ(8,-) ITMX
C!!!  COMPUTE SOURCE SPACING.
      DELS=(SMAX-SMIN)/NS
      WRITE(8,23)
23    FORMAT(' IS THE PATTERN DATA TO BE INPUT IN DECIBELS
     2(T OR F)?' )
      READ(8,-) LDB
      WRITE(8,3)
3     FORMAT(' INPUT FILE NAME OF PATTERN DATA POINTS: ')
      CALL RDFLNM(IFILE,IUSER)
      CALL ASSIGN(IFILE,IUSER,7)
      READ(7,-) MPMX
      READ(7,-) (PH(M),HD(M),M=1,MPMX)
C!!!  CONVERT DECIBEL PATTERN VALUES TO FIELD VALUES.
      IF(.NOT.LDB) GO TO 24
      DO 25 M=1,MPMX
25    HD(M)=10.**(.05*HD(M))
```

```
   24 CONTINUE
      DO 5 M=1,MPMX
    5 PH(M)=180.-PH(M)
C!!!  COMPUTE MATRIX ELEMENTS FOR SOURCE MATRIX T.
      DO 4 N=1,NS
      S=SMIN+(N-0.5)*DELS
      DO 4 M=1,MPMX
      PHR=PH(M)*RPD
    4 HS(M,N)=HPLN(S,PHR)
C!!!  SET INITIAL ZERO PHASE AND COMPUTE NORMALIZATION FOR
C!!!  ERROR CRITERION (ER)
      HOS=0.
      DO 10 M=1,MPMX
      PHAR(M)=0.
   10 HOS=HOS+HD(M)*HD(M)
C!!!  COMPUTE MATRIX ELEMENTS
      DO 11 NI=1,NS
      DO 11 NJ=1,NS
      TS=(0.,0.)
      DO 12 M=1,MPMX
   12 TS=TS+CONJG(HS(M,NI))*HS(M,NJ)
   11 T(NI,NJ)=TS
      WRITE(8,22)
   22 FORMAT(' IS CRT DISPLAY TO BE USED(T OR F)?')
      READ(8,-) LVISD
      IF(.NOT.LVISD) GO TO 44
C!!!  SET UP CRT,PLOT GRID,AND DESIRED VALUES
      CALL CRTON
      CALL CRTPTS(IBUF,10,3)
      CALL BRPLOT(CRTPLT)
      CALL GRID
      HMAX=0.
      DO 20 M=1,MPMX
   20 IF(HD(M).GT.HMAX) HMAX=HD(M)
      DO 21 M=1,MPMX
      HPLT=20.*ALOG10(HD(M)/HMAX)
      IF(HPLT.LT.-40.) HPLT=-40.
      HMX=(40.+HPLT)*2.5/40.
      PHR=PH(M)*RPD
      PHR=PHR-0.5*PI
      XPLT=HMX*SIN(PHR)
      YPLT=HMX*COS(PHR)
   21 CALL SYMBOL(XPLT,YPLT,0.025,11,0.,-1)
C!!!  GET ADDRESS OF GRID AND DESIRED VALUE TO ERASE PLOT
C!!!  DATA.
      CALL INFO(XPLT,YPLT,XO,YO,FACT,ITEN,IADR)
   44 WRITE(8,38)
   38 FORMAT(' INCREMENT DATA PLOTTED BY=? ')
```

```
      READ(8,-) NPLTMX
      NPLT=NPLTMX
      MI=1
      MF=MPMX
      MS=1
      TESTN=1.
      DO 821 M=MI,MF,MS
  821 HLAST(M)=(0.,0.)
      LPHASE=.TRUE.
      DELT=.04
      DELTN=-DELT
C!!!  ITERATE ON RESULTS
      DO 31 IT=1,ITMX
      NPLT=NPLT+1
C!!!  COMPUTE COMPLEX FIELD POINT VALUES.
      DO 32 M=MI,MF,MS
      HITM(M)=HD(M)*CEXP(CJ*PHAR(M))
C!!!  COMPUTE UPDATED FIELD POINT VALUES
C!!!  BASED ON INCREMENTAL PHASE CHANGE
C!!!  BETWEEN LAST AND PRESENT ITERATION.
      HITM(M)=HLAST(M)+TESTN*(HITM(M)-HLAST(M))
   32 HLAST(M)=HITM(M)
C!!!  COMPUTE SOURCE VECTOR.
      DO 33 N=1,NS
      F(N)=(0.,0.)
      DO 33 M=MI,MF,MS
   33 F(N)=F(N)+HITM(M)*CONJG(HS(M,N))
      DO 34 NJ=1,NS
      DO 34 NI=1,NS
      NN=(NJ-1)*NS+NI
   34 C(NN)=T(NI,NJ)
C!!!  SOLVE SIMULTANEOUS EQUATIONS.
      CALL CGELG(F,C,NS,1,1.E-6,IER)
      IF(IER.NE.0) WRITE(8,35) IER
   35 FORMAT(' ERROR IN GELG:IER=',I2)
      IF(LPHASE) GO TO 521
      DO 534 NJ=1,NS
      DO 534 NI=1,NS
      NN=(NJ-1)*NS+NI
  534 C(NN)=T(NI,NJ)
C!!!  COMPUTE UPDATED FIELD POINT DIFFERENCE VALUES
C!!!  BASED ON INCREMENTAL MAGNITUDE CHANGE BETWEEN
C!!!  ITERATION JUST COMPLETED AND PREVIOUS ITERATION.
      DO 532 M=MI,MF,MS
      TS=(0.,0.)
      DO 552 N=1,NS
  552 TS=TS+F(N)*HS(M,N)
      PHARN=CATAN2(TS)
      HMN=CABS(TS)
```

```
532   HITM(M)=HD(M)*CEXP(CJ*PHARN)-HMN*CEXP(CJ*PHAR(M))
C!!!  COMPUTE INCREMENTAL CHANGE IN SOURCES
C!!!  DUE TO CHANGE IN FIELD POINT VALUES.
      DO 533 N=1,NS
      FF(N)=(0.,0.)
      DO 533 M=MI,MF,MS
533   FF(N)=FF(N)+HITM(M)*CONJG(HS(M,N))
      CALL CGELG(FF,C,NS,1,1.E-6,IER)
      IF(IER.NE.0) WRITE(8,35) IER
C!!!  ADD INCREMENTAL CHANGE IN SOURCES TO
C!!!  PREVIOUS SOURCE VALUES.
      DO 522 N=1,NS
522   F(N)=F(N)+FF(N)
521   IF(.NOT.LVISD) GO TO 41
C!!!  COMPUTE TOTAL PATTERN.
      IF(NPLT.LT.NPLTMX) GO TO 41
      DO 40 IP=0,360
      ID=IP+1
      PHR=IP*RPD
      HIT(ID)=(0.,0.)
      DO 40 N=1,NS
      S=SMIN+(N-0.5)*DELS
40    HIT(ID)=HIT(ID)+F(N)*HPLN(S,PHR)
      CALL ERASE(IADR)
      CALL CRTPLT(4.25,4.25,-3)
      CALL POLPLT(HIT)
41    FNS=0.
      HMS=0.
      HHS=0.
      DO 50 N=1,NS
50    FNS=FNS+CABS(F(N))**2
      DO 51 M=1,MPMX
      TS=(0.,0.)
      DO 52 N=1,NS
52    TS=TS+F(N)*HS(M,N)
      PHAR(M)=CATAN2(TS)
      HM=CABS(TS)
      HMS=HMS+HM*HM
51    HHS=HHS+(HM-HD(M))**2
      ER=HHS/HOS
      QR=MPMX*FNS/HMS
      WRITE(8,-) IT,ER,QR
      IF(IT.LE.5) DELTN=-DELT
      DELTN=DELTN+DELT
      IF(ER.GT.ERLAST)DELTN=DELTN*0.5
      ERLAST=ER
      IF(IT.GE.5)LPHASE=.FALSE.
      TESTN=1.+DELTN
      IF(TESTN.GT.2.) TESTN=2.
      IF(NPLT.LT.NPLTMX) GO TO 1031
      WRITE(8,723)TESTN
723   FORMAT(' WEIGHTING FACTOR= ',F10.5)
```

```
        WRITE(6,-) IT
        ICMAX=0
        CURMAX=0.
        DO 643 I=1,NS
        IF(CABS(F(I)).LT.CURMAX) GO TO 643
        CURMAX=CABS(F(I))
        ICMAX=I
  643   CONTINUE
        DO 46 I=1,NS
        CURM=CABS(F(I)/F(ICMAX))
        CURP=DPR*CATAN2(F(I)/F(ICMAX))
  46    WRITE(6,-) I,CURM,CURP
  1031  IF(NPLT.GE.NPLTMX) NPLT=0
        IF(IT.EQ.1)NPLT=1
  31    CONTINUE
* 9898  CALL ESC($9999)
  C!!!  COMPUTE TOTAL PATTERN AFTER COMPLETION
  C!!!  OR TERMINATION OF ITERATION LOOP.
        DO 45 IP=0,360
        ID=IP+1
        PHR=IP*RPD
        HIT(ID)=(0.,0.)
        DO 45 N=1,NS
        S=SMIN+(N-.5)*DELS
  45    HIT(ID)=HIT(ID)+F(N)*HPLN(S,PHR)
  C!!!  WRITE COMPUTED PATTERN VALUES INTO
  C!!!  PERMANENT FILE NAMED SYNSIS.
*       CALL ASSIGN(6HSYNSIS,0.,1)
*       WRITE(1) HIT
*       WRITE(8,9899)
* C!!!  PLOT COMPUTED PATTERN AND MEASURED PATTERN
* C!!!  VALUES FROM WHICH PATTERN WAS COMPUTED.
* 9899  FORMAT (' PEN PLOT DESIRED(T OR F)?')
*       READ(8,-) LOG
*       IF(.NOT.LOG) GO TO 9999
*       IF(.NOT.LVISD) GO TO 9376
*       CALL PLOT(0.,0.,-3)
*       CALL PLOT(0.,0.,999)
* 9376  CALL PLOTS(IBUF,512,3)
*       CALL BRPLOT(PLOT)
*       CALL GRID
*       HMAX=0.
*       DO 720 M=1,MPMX
* 720   IF(HD(M).GT.HMAX) HMAX=HD(M)
*       DO 721 M=1,MPMX
*       HPLT=20.*ALOG10(HD(M)/HMAX)
*       IF(HPLT.LT.-40.) HPLT=-40.
*       HMX=(40.+HPLT)*2.5/40.
*       PHR=PH(M)*RPD
```

```
      PHR=PHR-0.5*PI
      XPLT=HMX*SIN(PHR)
      YPLT=HMX*COS(PHR)
721   CALL SYMBOL(XPLT,YPLT,0.025,11,0.,-1)
      CALL POLPLT(HIT)
      CALL PLOTS(IBUF,512,3)
      LSOR=.TRUE.
      DO 786 IP=0,360
      ID=IP+1
      PHR=IP*RPD
      HIT(ID)=(0.,0.)
      DO 786 N=1,NS
      S=SMIN+(N-.5)*DELS
786   HIT(ID)=HIT(ID)+F(N)*HPLN(S,PHR)
      CALL GRID
      CALL POLPLT(HIT)
9999  CALL EXIT
      END
C!!!  **** END OF MAIN PROGRAM ****
      SUBROUTINE GRID
      DATA PI,TPI,DPR/3.14159265,6.2831853,57.29577958/
      RP=2.5
      CALL PLOT(4.25,4.25,-3)
C!!!  POLAR GRID
      DO 110 I=1,4
      RG=RP*I/4.
      CALL PLOT(RG,0.,3)
      DO 110 J=0,360,2
      ANG=J/DPR
      XX=RG*COS(ANG)
      YY=RG*SIN(ANG)
 110  CALL PLOT(XX,YY,2)
      DO 112 I=1,6
      ANG=(I-1)*PI/6.
      ANGS=ANG+PI
      ANGF=ANG
      IF(I.EQ.2*(I/2)) GO TO 111
      ANGS=ANG
      ANGF=ANG+PI
 111  CONTINUE
      XX=RP*COS(ANGS)
      YY=RP*SIN(ANGS)
      CALL PLOT(XX,YY,3)
      XX=RP*COS(ANGF)
      YY=RP*SIN(ANGF)
 112  CALL PLOT(XX,YY,2)
      RETURN
      END
      SUBROUTINE POLPLT(ET)
      COMPLEX ET(361)
```

```
      DATA PI,TPI,DPR/3.14159265,6.2831853,57.29577958/
      RP=2.5
      EMX=0.
      DO 101 IP=0,360
      I=IP+1
      EM=CABS(ET(I))
      IF(EM.GT.EMX) EMX=EM
  101 CONTINUE
C!!!  PATTERN PLOT
      DO 120 IP=0,360
      I=IP+1
      ETM=CABS(ET(I))/EMX
      IF(ETM.LT.0.01) ETM=0.01
      RD=20.*ALOG10(ETM)
      IF(RD.LT.-40.) RD=-40.
      RD=RP*(RD+40.)/40.
  125 CONTINUE
      ANG=IP/DPR
      ANG=ANG-0.5*PI
      XX=RD*SIN(ANG)
      YY=RD*COS(ANG)
      IPEN=2
      IF(I.EQ.1) IPEN=3
  120 CALL PLOT(XX,YY,IPEN)
      CALL PLOT(4.25,-5.5,-3)
  130 CONTINUE
      CALL PLOT(0.,0.,999)
      RETURN
      END
      COMPLEX FUNCTION HPLN(S,PHR)
      COMPLEX CJ,DC,HI
      COMMON/PLAT/W,LSOR
      LOGICAL LSOR
      DATA CJ/(0.,1.)/
      DATA PI,TPI,DPR/3.14159265,6.2831853,57.29577958/
      HI=CEXP(-CJ*TPI*S)/SQRT(S)
      HPLN=CEXP(CJ*TPI*S*COS(PHR))
      IF(LSOR) RETURN
      CALL DI(DC,S,PHR,1.,2.)
      IF(PHR.GT.PI) HPLN=(0.,0.)
      HPLN=HPLN+HI*DC
      HI=CEXP(-CJ*TPI*(W-S))/SQRT(W-S)
      PHR2=PI-PHR
      IF(PHR2.LT.0.) PHR2=TPI+PHR2
      CALL DI(DC,W-S,PHR2,1.,2.)
      HPLN=HPLN+HI*DC*CEXP(CJ*TPI*W*COS(PHR))
      RETURN
      END
      SUBROUTINE DI(DIR,R,ANGR,SBO,FN)
```

```
C *** INCIDENT (BET=PH-PHP) OR REFLECTED (BET=PH+PHP) ***
C *** PART OF WEDGE DIFFRACTION COEFFICIENT ***
      COMPLEX COM,EX,UPPI,UNPI,FA,DIR
      COMPLEX TOP
      COMMON/CONST/TOP
      DATA PI,TPI,DPR/3.14159265,6.2831853,57.29577958/
      DEM=2.*TPI*FN*SBO
      COM=TOP/DEM
      SQR=SQRT(TPI*R)
      DNS=(PI+ANGR)/(2.0*FN*PI)
      SGN=SIGN(1.,DNS)
      N=IFIX(ABS(DNS)+0.5)
      DN=SGN*N
      A=ABS(1.0+COS(ANGR-2.0*FN*PI*DN))
      BOTL = 2.0*SQRT(ABS(R*A))
      EX=CEXP(CMPLX(0.0,TPI*R*A))
      CALL FRNELS (C,S,BOTL)
      C=SQRT(PI/2.0)*(0.5-C)
      S= SQRT(PI/2.0)*(S-0.5)
      FA=CMPLX(0.,2.)*SQR*EX*CMPLX(C,S)
      RAG=(PI+ANGR)/(2.0*FN)
      TSIN=SIN(RAG)
      TS=ABS(TSIN)
      IF(TS.GT.1.E-5) GO TO 442
      COTA=-SQRT(2.0)*FN*SIN(ANGR/2.0-FN*PI*DN)
      IF(COS(ANGR/2.0-FN*PI*DN).LT.0.0) COTA=-COTA
      GO TO 443
  442 COTA=SQRT(A)*COS(RAG)/TSIN
  443 UPPI=COM*COTA*FA
      DNS=(-PI+ANGR)/(2.0*FN*PI)
      SGN=SIGN(1.,DNS)
      N=IFIX(ABS(DNS)+0.5)
      DN=SGN*N
      A=ABS(1.0+COS(ANGR-2.0*FN*PI*DN))
      BOTL = 2.0*SQRT(ABS(R*A))
      EX=CEXP(CMPLX(0.0,TPI*R*A))
      CALL FRNELS (C,S,BOTL)
      C=SQRT(PI/2.0)*(0.5-C)
      S= SQRT(PI/2.0)*(S-0.5)
      FA=CMPLX(0.,2.)*SQR*EX*CMPLX(C,S)
      RAG=(PI-ANGR)/(2.0*FN)
      TSIN=SIN(RAG)
      TS=ABS(TSIN)
      IF(TS.GT.1.E-5) GO TO 542
      COTA= SQRT(2.0)*FN*SIN(ANGR/2.0-FN*PI*DN)
      IF(COS(ANGR/2.0-FN*PI*DN).LT.0.0) COTA=-COTA
      GO TO 123
  542 COTA=SQRT(A)*COS(RAG)/TSIN
  123 UNPI=COM*COTA*FA
      DIR=UPPI+UNPI
```

```
      RETURN
      END
      SUBROUTINE FRNELS(C,S,XS)
C     THIS IS THE FRESNEL INTEGRAL SUBROUTINE WHERE THE INTEGRAL IS FROM
C     U=0 TO XS, THE INTEGRAND IS EXP(-J*PI/2.*U*U),AND THE OUTPUT IS
C     C(XS)-J*S(XS).
      DIMENSION A(12),B(12),CC(12),D(12)
      DATA A/1.595769140,-0.000001702,-6.808568854,-0.000576361,6.920691
     *902,-0.016898657,-3.050485660,-0.075752419,0.850663781,-0.0256390 4
     *1,-0.150230960,0.034404779/
      DATA B/-0.000000033,4.255387524,-0.000092810,-7.780020400,-0.00952
     *0895,5.075161298,-0.138341947,-1.363729124,-0.403349276,0.7022 2201
     *6,-0.216195929,0.019547031/
      DATA CC/0.,-0.024933975,0.000003936,0.005770956,0.000689892,-0.009
     *497136,0.011948809,-0.006748873,0.000246420,0.002102967,-0.0012179
     *30,0.000233939/
      DATA D/0.199471140,0.000000023,-0.009351341,0.000023006,0.00485146
     *6,0.001903218,-0.017122914,0.029064067,-0.027928955,0.016497308,-0
     *.005598515,0.000838386/
      DATA PI/3.14159265/
      IF(XS.LE.0.0) GO TO 414
      X=XS
      X = PI*X*X/2.0
      FR=0.0
      FI=0.0
      K=13
      IF(X-4.0) 10,40,40
10    Y=X/4.0
20    K=K-1
      FR=(FR+A(K))*Y
      FI=(FI+B(K))*Y
      IF(K-2) 30,30,20
30    FR=FR+A(1)
      FI=FI+B(1)
      C=(FR*COS(X)+FI*SIN(X))*SQRT(Y)
      S=(FR*SIN(X)-FI*COS(X))*SQRT(Y)
      RETURN
40    Y=4.0/X
50    K=K-1
      FR=(FR+CC(K))*Y
      FI=(FI+D(K))*Y
      IF(K-2) 60,60,50
60    FR=FR+CC(1)
      FI=FI+D(1)
      C=0.5+(FR*COS(X)+FI*SIN(X))*SQRT(Y)
      S=0.5+(FR*SIN(X)-FI*COS(X))*SQRT(Y)
      RETURN
414   C=-0.0
      S=-0.0
      RETURN
      END
```